



저작자표시-비영리-변경금지 2.0 대한민국

이용자는 아래의 조건을 따르는 경우에 한하여 자유롭게

- 이 저작물을 복제, 배포, 전송, 전시, 공연 및 방송할 수 있습니다.

다음과 같은 조건을 따라야 합니다:



저작자표시. 귀하는 원저작자를 표시하여야 합니다.



비영리. 귀하는 이 저작물을 영리 목적으로 이용할 수 없습니다.



변경금지. 귀하는 이 저작물을 개작, 변형 또는 가공할 수 없습니다.

- 귀하는, 이 저작물의 재이용이나 배포의 경우, 이 저작물에 적용된 이용허락조건을 명확하게 나타내어야 합니다.
- 저작권자로부터 별도의 허가를 받으면 이러한 조건들은 적용되지 않습니다.

저작권법에 따른 이용자의 권리는 위의 내용에 의하여 영향을 받지 않습니다.

이것은 [이용허락규약\(Legal Code\)](#)을 이해하기 쉽게 요약한 것입니다.

[Disclaimer](#)

이학박사 학위논문

*Listeria monocytogenes*에 대한 선천 면
역반응에서 DRG2의 역할 연구

**DRG2 is required for innate immunity against
Listeria monocytogenes infection**

울 산 대 학 교 대 학 원

생 명 과 학 과

이 언 화






**DRG2 is required for innate immunity
against *Listeria monocytogenes* infection**

지도교수 박정우

이 논문을 이학박사 논문으로 제출함
2022년 7월

울산대학교 대학원
생명과학과
이언화

이언화의 이학박사 학위논문을 인준함

심사위원장	최혜선	
심사위원	이병주	
심사위원	소홍섭	
심사위원	이정진	
심사위원	박정우	

울 산 대 학 교 대 학 원

2022 년 6 월

**DRG2 is required for innate immunity
against *Listeria monocytogenes* infection**

Supervisor: Prof. Dr. Jeong Woo Park

**A thesis submitted to
the Graduate School of University of Ulsan
in partial fulfillment of the requirements
for the degree of**

Doctor of Science

by

Unnhwa Lee

Department of Biological Science

Ulsan, Korea

July, 2022

CONTENTS

I.	ABSTRACT	6
II.	INTRODUCTION	7
III.	MATERIALS AND METHODS	9
1.	Mice and Animal Research Ethics	9
2.	Bacterial infections and enumeration of bacterial burdens	9
3.	Analysis of immune cell infiltration in the peritoneum and in circulation	9
4.	Bone Marrow-Derived Macrophage (BMM) Culture and Differentiation	10
5.	In vitro stimulation of BMMs	10
6.	Macrophage migration assay in vitro	10
7.	ChIP assays	11
8.	Confocal microscopy of NF- κ B nuclear localization	11
9.	Nuclear fractionation	12
10.	SDS-PAGE and immunoblotting	12
11.	Determination of Inflammatory Cytokine Levels	12
12.	Quantitative Real-Time RT-PCR	12
13.	Intracellular staining and flow cytometry	13
14.	Measurement of bacterial association and entry into host cells	13
15.	Growth of <i>L. monocytogenes</i> in macrophage	14
16.	Generation of macrophage specific DRG2 KO mice	14
17.	Bone marrow transplantation	14
18.	Depletion of macrophages in vivo by clodrolip	15
19.	Depletion of macrophages using clodronate liposomes reconstitution of macrophages in mice	15
20.	Histopathology	15

21. Statistics-----	16
IV. RESULTS-----	17
1. <i>DRG2</i> ^{-/-} macrophages shows intrinsic defects in expression of inflammatory cytokines and chemokines. -----	17
2. <i>DRG2</i> ^{-/-} macrophages shows intrinsic defects in production of inflammatory cytokines. -----	17
3. DRG2 deficiency does not affect the number and the frequency of splenic and lymphatic immune cells-----	18
4. Dexamethasone-induced reduction of inflammatory cytokines was independent of DRG2-----	18
5. DRG2 deficiency inhibits NF-κB pathway-----	20
6. DRG2 deficiency delayed monocyte recruitment to the peritoneal cavity in <i>L. monocytogenes</i> -infected mice-----	21
7. DRG2 deficiency does not affect the phagocytosis of <i>L. monocytogenes</i> by macrophages-----	21
8. DRG2 deficiency increases sensitive to <i>L. monocytogenes</i> infection-----	22
9. Proinflammatory cytokine level following <i>L. monocytogenes</i> infection in WT and <i>DRG2</i> ^{-/-} mice varies with time point-----	24
10. <i>DRG2</i> ^{-/-} neutrophils shows defect in production of inflammatory cytokines-----	25
11. <i>DRG2</i> depletion enhances the expression of inflammatory cytokines and chemokines in endothelial cells-----	25
12. Macrophage DRG2 depletion leads to the susceptibility of <i>L. monocytogenes</i> infection-----	26

13. Macrophage depletion with Clodrolip dramatically increases sensitivity to <i>L. monocytogenes</i> -----	27
14. Cells of γ -irradiated recipient mice determine the sensitivity to <i>L. monocytogenes</i> infection in bone marrow graft experiment-----	28
15. Reconstitution of clodronate-treated mice with either macrophages from WT or <i>DRG2</i> $-/-$ mice does not protect mice from <i>L. monocytogenes</i> infection-----	28
V. DISCUSSION-----	55
VI. REFERENCES-----	58

LIST OF FIGURES

Figure 1. DRG2 ^{-/-} macrophages shows intrinsic defect in inflammatory cytokine and chemokine expression -----	30
Figure 2. DRG2 ^{-/-} shows intrinsic defect in inflammatory cytokine production---	31
Figure 3. Dexamethasone-induced reduction of inflammatory cytokines was independent of DRG2-----	32
Figure 4. DRG2 ^{-/-} macrophages shows intrinsic defect in NF-κB activation pathway and inflammatory cytokine production-----	33
Figure 5. DRG2 deficiency attenuates the migration of monocytes and macrophages-----	35
Figure 6. DRG2 ^{-/-} mice are sensitive to <i>i.p.</i> infection with <i>L. monocytogenes</i> ----	37
Figure 7. DRG2 ^{-/-} mice are sensitive to <i>i.v.</i> infection with <i>L. monocytogenes</i> ----	38
Figure 8. Cytokine production following <i>L. monocytogenes</i> infection in WT and DRG2 ^{-/-} mice-----	39
Figure 9. DRG2 ^{-/-} neutrophils shows defect in production of inflammatory cytokines-----	40
Figure 10. DRG2 depletion enhances the expression of inflammatory cytokines and chemokines in endothelial cells-----	41
Figure 11. DRG2 MKO mice are sensitive to <i>i.p.</i> infection with <i>L. monocytogenes</i> -----	42
Figure 12. Macrophage depletion with Clodrolip dramatically increases sensitivity to <i>L. monocytogenes</i> -----	43
Figure 13. Cells of γ-irradiated recipient mice determine the sensitivity to <i>L. monocytogenes</i> infection in bone marrow graft experiment-----	45
Figure 14. Reconstitution of Clodronate-treated mice with either macrophages from WT or DRG2 KO mice does not protect mice from	

<i>L. monocytogenes</i> infection-----	46
Supplementary Figure S1. Body weight of wild-type and DRG2 ^{-/-} mice-----	47
Supplementary Fig.S2. Western blot analysis for the expression of DRG2 protein in lymph node, thymus, and spleen of wild-type and DRG2 ^{-/-} mice-----	48
Supplementary Fig.S3. DRG2 deficiency does not affect the uptake and killing of bacteria by macrophages-----	49
Supplementary Fig.S4. DRG2 deficiency does not affect the popularities of immune cells in lymphoid organs-----	50
Supplementary Fig. S5. DRG2 deficiency does not affect the popularities of immune cells in lymphoid organs-----	53
Supplementary Figure S6. Body weight of DRG2 ^{fl/fl} LysM Cre ^{-/-} and DRG2 ^{fl/fl} LysM Cre ^{+/-} mice-----	54

Abstract

The ability of macrophages to produce inflammatory cytokines plays a pivotal role in the innate immune response. Here we demonstrated that developmentally regulated GTP binding protein 2 (DRG2)^{-/-} macrophages are intrinsically defective in migration and inflammatory cytokine production. DRG2^{-/-} macrophages showed increased inhibitory phosphorylation of GSK3 β and decreased transcriptional activity of NF- κ B upon infection with *Listeria monocytogenes*. *L. monocytogenes* is a pathogen causing listeriosis that can be serious for individuals with impaired immune system. The innate immune response is critical for the control of early *L. monocytogenes* infection. Here, we report that DRG2 is a major regulator of innate immune response against *L. monocytogenes* infection. Using a DRG2^{-/-} mouse, we determined that DRG2 deficiency decreased survival upon *L. monocytogenes* infection. Additionally, in DRG2 macrophage specific KO mice, compared to DRG2^{fl/fl} mice, decreased survival upon *L. monocytogenes* infection. Lastly, DRG2^{-/-} macrophages showed increase in the inhibitory phosphorylation of GSK3 β and decrease in the transcriptional activity of NF- κ B upon *L. monocytogenes* infection. Our findings reveal a novel function of DRG2 in the cytokine production of immune cells and control of *L. monocytogenes* infection and host resistance.

Introduction

Developmentally regulated GTP-binding proteins (DRGs) are a novel class of evolutionarily conserved GTP-binding proteins and constitute a subfamily of the GTPase superfamily (1). The DRG subfamily contains two closely related proteins, DRG1 and DRG2 (2). It was shown that overexpression of DRG2 suppresses the growth of Jurkat T cells through cell cycle arrest at the G2/M phase (3,4) and inhibits T_H17 differentiation and ameliorates experimental autoimmune encephalomyelitis in mice (5). These suggest that DRG2 may play important roles in controlling immune response. However, the precise functional roles of DRGs in immune response remain poorly understood. Recently, we reported that DRG2-depleted cells showed defects in Rab5 deactivation on endosomes and recycling of endosomes to the plasma membrane (6). In addition, we found that DRG2 deficiency increased Akt activity and thus decreased GSK3 β activity (7). Given the role of GSK3 β in inflammatory cytokine production during infection (8, 9, 10), it was hypothesized that cytokines would be reduced in DRG2-deficient macrophages. Glycogen synthase kinase 3 β (GSK3 β) is a serine-threonine kinase that are broadly expressed and constitutively active in most cell types, including cells of the immune response (8, 9, 10). GSK3 β has been shown to activate or inhibit NF- κ B depending on the cell type and experimental conditions (11, 12, 13, 14, 15, 16). In naive macrophages, GSK3 β is constitutively active and can augment the production of pro-inflammatory cytokines after acute stimulation (8, 9, 10). GSK3 β has been reported to be required for recruitment of p65 to promoters of a subset of NF- κ B target genes (12) and target gene expression (17). The pro-inflammatory function for GSK3 has been linked to GSK3-mediated phosphorylation and stabilization of NF- κ B, B-cell lymphoma 3-encoded protein (BCL-3) (a transcriptional co-activator of NF- κ B p50 homodimer) (18, 19), and NEMO (20). NF- κ B plays a critical role in the inflammatory response (21). In resting cells NF- κ B is rendered inactive within the cytoplasm through association with inhibitory I κ B proteins. Various inflammatory stimuli can trigger the activation of the I κ B kinase (IKK) complex which consists of the regulatory subunit NF- κ B Essential Modifier (NEMO/IKK γ) and two catalytic subunits (IKK α and IKK β) (22). The activated IKK phosphorylates I κ B, liberating NF- κ B for nuclear translocation and activating pro-inflammatory gene expression (23).

The Gram-positive bacterium *Listeria monocytogenes* is a food-borne, intracellular pathogen that primarily affects the elderly, pregnant women, newborns, and people with weakened immune systems and causes listeriosis with a high mortality rate (24, 25). The murine model of listeriosis has shown that innate immunity controls the early response of the infection and is critical for survival (26). *L. monocytogenes* is detected by multiple innate immune signaling pathways during infection (27). Following engulfment by macrophages and dendritic cells, the bacteria reside within phagosomes where they are detected by Toll-Like Receptors (TLRs), resulting in the activation of MyD88-dependent response genes (28). Analyses of the transcriptional host responses in cells infected with *L. monocytogenes* have shown that NF- κ B signaling pathways predominantly contribute to produce pro-inflammatory cytokines against a *Listeria* infection (29, 30, 31).

Importantly, we found that DRG2 deficiency inhibited GSK3 β activity, leading to decrease in NF- κ B activity and inflammatory cytokine and chemokine production in macrophages. Consistent with the in vitro results, it was confirmed that the initial inflammatory response and survival rate were reduced when *L. monocytogenes* was injected intraperitoneally in DRG2-deficient mice in the *L. monocytogenes* infection model. These studies demonstrated that DRG2 contributes to protection against *L. monocytogenes* infection by regulating the NF- κ B signaling pathways and inflammatory cytokine production in macrophages

Materials and Methods

Mice and Animal Research Ethics

DRG2^{-/-} mice were described previously (6). C57BL/6 (C57BL/6NCrljBgi) mice were purchased from Orientbio (Sungnam, Korea). *DRG2*^{fl/fl} *LysM-Cre* (32), were on a C57BL/6 genetic background. *DRG2*^{fl/fl} *LysM-Cre* were kept heterozygous for the Cre recombinase allele to obtain control *DRG2*^{fl/fl} or conditional myeloid-knockout (*DRG2* MKO) littermates. Mice were bred in the animal facility at the University of Ulsan and were born and housed in the same room under specific pathogen-free conditions. All mice were handled in accordance with the guidelines of the Institutional Animal Care and Use Committee of the University of Ulsan. All animal procedures were approved by the Institutional Animal Care and Use Committee of Meta-inflammation Research Center. All surgery was performed under sodium pentobarbital anesthesia, and all efforts were made to minimize suffering.

Bacterial infections and enumeration of bacterial burdens

Male mice were lethally infected *i.p.*(intraperitoneally) with 5.5×10^4 or *i.v.*(intravenously) with 9.0×10^3 L. monocytogenes per g of body weight. Mice were weighed and monitored daily for mortality for up to 10 days. Differences in survival were analyzed by the Mantel–Cox test. To study bacterial clearance, mice were euthanized at days 2 and 3 after infection, liver and spleen tissue were homogenized and bacterial burdens were enumerated by serial dilution on brain–heart infusion (BHI) agar plates.

Analysis of immune cell infiltration in the peritoneum and in circulation

Wild-type and *DRG2*^{-/-} mice were infected *i.p.* with 1.3×10^6 C.P.U. of *L. monocytogenes*. At 6 h, 1 day, 2 days and 3 days after infection, cells were collected by peritoneal lavage in either 1 ml IMDM (for cytokines analysis) or 10 ml IMDM (for total cell recruitment to the cavity) on ice. Cells were washed twice with PBS and surface-stained for anti-CD11b (Ebioscience; 11-0112-82), anti-(Gr1) Ly6G

(Ebioscience; clone 12-5931-82) Data were acquired on a FACSCalibur (BD Biosciences) and analyzed with WinMDI 2.9 software.

Bone Marrow-Derived Macrophage (BMM) Culture and Differentiation

For the BMM cultures, bone marrow was isolated from the femurs and tibias of WT and *DRG2 KO* mice and cultured in minimum essential medium alpha (a-MEM) supplemented with 10% fetal bovine serum (FBS). The cells were plated and cultured overnight in the presence of macrophage colony-stimulating factor (M-CSF, 10 ng/ml). The non-adherent cells were collected and cultured for 3 days in the presence of M-CSF (10 ng/ml). The floating cells were removed, and the adherent cells were used as BMMs.

In vitro stimulation of BMMs

BMDMs were seeded in 12-well plates at 1×10^6 cells/well. The following day, the medium was exchanged with fresh antibiotic-free medium. Cells were then stimulated with *L. monocytogens* at an MOI of 10 in RPMI-1640, 10 ng/ml LPS, or 1 μ g/ml FSL-1 or 2 μ g/ml poly(I:C). At indicated time points, supernatants were collected and analyzed for cytokines by ELISA. For western blot analysis, cells were harvested, washed in PBS, and then lysed in lysis buffer (50 mM Tris, pH 8.0, 150 mM NaCl, 1% Nonidet P-40, 0.5% sodium deoxycholate, 0.1% SDS) containing protease inhibitor cocktail (Roche) and PhosSTOP (Roche).

Macrophage migration assay in vitro

Macrophage migration was examined using a 24-well Transwell plate (Corning, Inc., NY, USA). Approximately 1×10^5 peritoneal macrophages in serum-free DMEM were placed on the upper chamber polycarbonate membrane. Migration was induced by adding 600 μ l of RPMI-1640 (Gibco, Invitrogen Corporation, UK), supplemented with 10% FBS (Sigma) and 30% L929 cell-conditioned medium to the lower chamber. After incubation at 37°C for 6 h or 24 h at 37 °C in a 5% CO₂ incubator, non-migratory cells were removed from the upper surface of the membrane by

scraping with cotton swabs. Migrated cells at the bottom of were fixed, stained with May-Giemsa, and counted at $\times 200$ magnification in five randomly chosen microscope fields per membrane.

ChIP assays

ChIP assays were performed using the EZ-Magna ChIP™ G Kit (Millipore). The chromatin was immunoprecipitated with anti-NF- κ B p65(NB100-2175, Novus), or isotype control antibody. DNA was amplified by PCR with the following primers: IL-6-p primers (5'- GACATGCTCAAGTGCTGAGTCAC -3' and 5'- AGATTGCACAATGTGACGTCG -3') which amplified the 143-bp region (-341 to -198) of the IL-6 promoter containing the binding site for c-Rel; IL-1 β -p primers (5'- TCCCTGGAAATCAAGGGGTGG -3' and 5'- TCTGGGTGTGCATCTACGTGCC -3') which amplified the 196-bp region (-347 to -151) of the IL-1 β promoter containing the binding site for c-Rel; TNF- α -p primers (5'-CTGATTGGCCCCAGATTG -3' and 5'-CTTCTGCTGGCTGGCTGT -3') which amplified the 266-bp region (-270 to -4), of the TNF- α promoter containing the binding site for RelA; IL-6-ORF primers (5'-CTGCTGAAAGCTAAGCTCGC-3' and 5'-ACACGGGCATCACC CGACTT-3') which amplified the 91-bp region (ORF 87–177) of the DRG2 ORF.

Confocal Microscopy of NF- κ B Nuclear Localization

Cells were stimulated with FSL-1 for 1 h, washed three times with ice-cold PBS and fixed with 4% paraformaldehyde (Sigma). NF- κ B was stained using anti- NF- κ B p65 antibody (Novus) and goat anti-rabbit IgG Alexa Fluor 488 (Invitrogen). Nuclei were stained using 4',6-diamidino-2-phenylindole (DAPI) (Sigma-Aldrich). Confocal images were acquired in sequential mode using a 100 \times Plan Aplanachromat NA/1.4 oil objective and the appropriate filter combination on an Olympus 1000/1200 laser-scanning confocal system. All images were saved as TIFF files, and their contrast was adjusted with Image J (v1.19m).

Nuclear fractionation

Cells were stimulated with FSL-1 at indicated time points. Following the incubation periods, cytosolic and nuclear fractions were sequentially isolated using a cell fractionation kit (Thermo Scientific) according to the manufacturer's protocol. Purity of fractions was determined by Western blot analysis using specific nuclear and cytosolic markers.

SDS-PAGE and immunoblotting

Proteins in the cell lysates were resolved by SDS-PAGE, transferred onto Hybond-P membranes (Amersham Biosciences Inc.), and probed with appropriate dilutions of the following antibodies: anti-human DRG2 (Proteintech), anti-Akt (Cell signaling), anti-phospho-Akt (S473) (Cell signaling), anti-GSK3 β (Cell signaling), anti-phospho-GSK3 β (S9) (Cell signaling), anti-I κ B (Santa Cruz), anti-phospho-I κ B (Cell signaling), and anti- β -actin (Sigma). Immunoreactivity was detected using Pierce ECL Western blotting substrate (Thermo Scientific).

Determination of Inflammatory Cytokine Levels

The concentrations of TNF- α and IL-6 in sera, liver, peritoneal lavage, and cell culture supernatant were determined with DuoSet ELISA (enzyme-linked immunosorbent assay) Development Systems kits (R&D Systems, Minneapolis, MN). ELISA results were normalized with the use of a standard curve. Livers were homogenized in M-PER mammalian protein extraction reagent (Thermo scientific) and centrifuged to obtain supernatant fluids for ELISA. Total protein concentrations in the liver tissue homogenates were determined with bicinchoninic acid protein assay kit (Pierce Biotechnology).

Quantitative Real-Time RT-PCR

Total RNA was extracted from cells and the accessory lobe of lung of WT and DRG2 knockout mice with the use of the RNeasy Mini Kit (Qiagen, Hilden, Germany). For RNA kinetic analysis, 3 mg of DNase I-treated total RNA was reverse transcribed

with oligo-dT and Superscript II Reverse Transcriptase (Invitrogen, Carlsbad, CA) according to the manufacturer's instructions. RT-qPCR was performed by monitoring the increase in fluorescence in real time of SYBR Green dye (Qiagen) with the use of StepOnePlus Real-time PCR kits (Applied Biosystems, Foster City, CA) with the use of the following PCR primer pairs: glyceraldehyde-3-phosphate dehydrogenase, forward, 5'- GGGAAAGCCCATCACCATCT -3' and reverse, 5'- CGGCCTCACCCCATTTG -3'; IL-1 β , forward, 5'- TCGCTCAGGGTCACAAGAAA -3' and reverse, 5'- ATCAGAGGCAAGGAGGAAACAC -3'; IL-6, forward, 5'- CGATGATGCACTTGCAGAAA -3' and reverse, 5'- TGGAAATTGGGGTAGGAAGG -3'; and TNF- α , forward, 5'- AGACCCTCACACTCAGATCATCTTC -3' and reverse, 5'- TTGCTACGACGTGGGCTACA -3, CXCL1, forward, 5'- TCCAGAGCTTGAAGGTGTTGCC -3'; and reverse, 5'- AACCAAGGGAGCTTCAGGGTCA -3'; CXCL2, forward, 5'- CATCCAGAGCTTGAGTGTGACG -3'; and reverse, 5'- GGCTTCAGGGTCAAGGCAAACACT -3'.

Intracellular Staining and Flow Cytometry.

Single-cell suspensions were prepared from spleens, lymph nodes, peritoneal cavity of wild-type and DRG2^{-/-} mice. Cells were stained with anti-CD3-PerCP-Cy5, anti-CD4-FITC, anti-CD8-PE, anti-B220-FITC, anti-NK1.1-PE, anti-Ly6G(Gr-1), anti-CD11b-PE, anti-F4/80-FITC, anti-CD197(CCR7)-PerCP-Cy5.5 (eBioscience), and anti-CD206-PE antibodies (Biolegend). Data were acquired on a FACSCalibur (BD Biosciences) and analyzed with WinMDI 2.9 software.

Measurement of Bacterial Association and Entry into Host Cells

Bacteria were labeled, as previously described (33). Briefly, bacteria were incubated with 100 mM CFSE (Invitrogen) for 10 min at 37°C, washed in PBS, and immediately used for the in vitro infection of macrophages. BMDMs were seeded in a 48-well plate at 2.5×10^5 cells well⁻¹ and incubated at 37°C for 2 h in RPMI 1640 medium supplemented with 10% FBS. After being washed to remove nonadherent cells, adherent macrophages were infected with *L. monocytogenes* at a multiplicity

of infection (MOI) of 10 at 37°C for 1 h in FBS-free RPMI 1640 medium. Extracellular bacteria were eliminated from the analysis by adding trypan blue (0.2% final) prior to analysis as described (34). Cells with associating *L. monocytogenes* or phagocytosed *L. monocytogenes* were analyzed by flow cytometry and confocal microscopy. Extracellular fluorescence was then quenched using Trypan blue. The fluorescence of internalized *L. monocytogenes* was analyzed by flow cytometry.

Growth of *L. monocytogenes* in Macrophage

BMDMs were plated at 3×10^5 cells per well in 24-well tissue culture plates 24 h prior to infection. Cells were then infected with *L. monocytogenes* at an MOI of 1 in RPMI-1640. After 30 min of invasion at 37°C, cells were washed three times with phosphate-buffered saline (PBS) followed by the addition of RPMI-1640. At 60 min p.i., media was changed, and RPMI-1640 with 10% FBS containing 50 µg/ml gentamicin was added. Cells were then lysed at 2, 4, 6, and 8 hr p.i. with T.D.W.. Serial dilutions of the lysates were plated on BHI-agar plates and incubated at 37°C for 16 h for subsequent quantification of intracellular CFUs.

Generation of Macrophage Specific DRG2 KO Mice

DRG2^{fl/fl} mice were generated from Institut Clinique de la Souris (Cedex, France) and *LysM-Cre* mice were purchased from Jackson Laboratory (Bar Harbor, ME, USA). *DRG2^{fl/fl}* and *LysM-Cre* mice were crossed to obtain *DRG2 KO* mice. To avoid potential variations that could be contributed by gender and genetic background, male mice from the F2 generation, *DRG2^{fl/fl}/LysM-Cre^{+/-}* (*DRG2 MKO*) and *DRG2^{fl/fl}/LysM-Cre2/2* (*DRG2^{fl/fl}*), were used for the studies. All of the experimental animals used in this study were maintained under the protocol approved by the Animal Care and Use Committee of the University of Ulsan.

Bone Marrow Transplantation

Mice were transplanted according to a standard protocol described previously (67). Mice were administered sevotrim for a week before gamma irradiation. Briefly, recipients received 900 cGy split into two doses separated by 3 hours to

minimize GI toxicity. On the day of gamma irradiation, 1×10^7 cells were injected with bone marrow cells obtained from the donor mouse into the tail vein of the recipient mouse. To effectively immunological reconstruct the mice were bred for 21 days and then *L. monocytogenes* was injected *i.p.*

Depletion of Macrophages in Vivo by Clodrolip

For evaluation the efficiency of macrophages depletion induced by clodrolip, the mice were injected with clodrolip and PBS-liposome (LIPOSOMA), via *i.p.* (1mg/20g). The depletion of macrophages was confirmed by flow cytometry. Briefly, splenocytes of the mice were obtained 1 day after the injection with clodrolip. Subsequently, the cells were stained with APC-anti-mouse monoclonal antibodies F4/80 (BD Biosciences). These cells were analyzed by a FACSCalibur (BD Biosciences) and analyzed with WinMDI 2.9 software. Wild-type (WT) and *DRG2*^{-/-} mice (8-week-old, male) were injected *i.p.* with PBS-liposome and clodrolip of mouse body weight(1mg/20g). After 1 day wild-type (WT) and *DRG2*^{-/-} mice were infected *i.p.* with 5.5×10^4 *L. monocytogenes* per g of mouse body weight. Survival was monitored daily for 14 days.

Depletion of Macrophages Using Clodronate Liposomes Reconstitution of Macrophages in Mice

Macrophages were depleted by *i.p.* administration of 1mg/20g of clodrolip. For reconstituting the macrophage in clodrolip-treated mice, bone marrow cells were isolated from the hind limbs of naive mice. The non-adherent cells were collected and cultured for 3 days in the presence of M-CSF (10 ng/ml). The floating cells were removed, and the adherent cells were used as BMMs. Then the adherent cells were isolated using a cell scraper and collected by centrifugation. Bone marrow-derived macrophages (BMM) were washed, stained with anti-mouse monoclonal antibodies F4/80, and then examined by flow cytometry ($\geq 80\%$). The BMM were transferred by *i.v.* injection 1×10^6 cells/mouse to mice that received with clodrolip on days 3.

Histopathology

Liver tissues were fixed in 4% paraformaldehyde, embedded in paraffin, and cut into 5-mm thick sections. Longitudinal sections were stained with haematoxylin and

eosin and examined by a pathologist blinded to the experimental groups.

Statistics

An unpaired Student's t-test (two-tailed) or one-way ANOVA was used to determine significant difference, P values less than 0.05 were considered significant. The Kaplan-Meier curve and log-rank tests were used to compare survival between Wild-type and DRG2^{-/-} mice.

Results

***DRG2*^{-/-} macrophages shows intrinsic defects in expression of inflammatory cytokines and chemokines.**

We previously demonstrated that overexpression of DRG2 inhibits NF- κ B activity and IL-6 production in macrophages (5). We thus hypothesized, initially, that DRG2 deficiency will produce high levels of inflammatory cytokines. To determine whether *DRG2* deficiency intrinsically regulates the inflammatory cytokine expression in macrophages, BMDM from wild-type and *DRG2*^{-/-} mice were stimulated with live *L. monocytogenes*, *LPS* and *FSL-1* and analyzed for inflammatory cytokine and chemokine expression. *DRG2*^{-/-} BMDMs expressed significantly lower levels of TNF- α (Fig. 1A, 1F), IL-6 (Fig. 1B, 1G), IL-1 β (Fig. 1C, 1H), CXCL1 (Fig. 1D, 1I), and CXCL2 (Fig. 1E, 1J) after *L. monocytogenes* and LPS stimulation than wild-type BMDMs. We also analyzed the inflammatory cytokine and chemokine expression by wild-type and *DRG2*^{-/-} peritoneal macrophages after stimulation with FSL-1 (TLR2 ligand). Consistently, *DRG2*^{-/-} peritoneal macrophages stimulated with these TLR2 agonists produced significantly lower levels of TNF- α (Fig. 1K), IL-6 (Fig. 1L), IL-1 β (Fig. 1M), CXCL1 (Fig. 1N), and CXCL2 (Fig. 1O) than wild-type macrophages. These results suggest that *DRG2* deficiency reduces expression of inflammatory cytokines and chemokines from macrophages.

***DRG2*^{-/-} macrophages shows intrinsic defects in production of inflammatory cytokines.**

There are several TLRs that can stimulate macrophages, and the receptors that respond to it are different depending on the type of agonist (68).

To determine whether DRG2 deficiency intrinsically regulates the inflammatory cytokine production in macrophages, peritoneal macrophages from wild-type and *DRG2*^{-/-} mice were stimulated with several TLR ligands and analyzed for inflammatory cytokine production. We analyzed the inflammatory cytokine

production by wild-type and *DRG2*^{-/-} macrophages after stimulation with other TLR ligands such as heat killed *L. monocytogenes*, FSL-1 (TLR2 ligand), poly I:C (TLR3 ligand), and LPS (TLR4 ligand). *DRG2*^{-/-} macrophages stimulated with these TLR agonists produced significantly lower levels of TNF- α (Fig. 2A) and IL-6 (Fig. 2B) than wild-type macrophages. These results suggest that DRG2 deficiency inhibits the production of inflammatory cytokines from macrophages regardless of the type of TLR.

DRG2 deficiency does not affect the number and the frequency of splenic and lymphatic immune cells.

To determine whether DRG2 deficiency affect immune cells populations, we analyzed the total cellularity of the spleen and the mesenteric lymph nodes in wild-type and *DRG2*^{-/-} mice 48 h after *L. monocytogenes* infection. Flow cytometry analysis of different subsets of immune cells showed no significant difference in the numbers and frequencies of CD4⁺, CD8⁺ T cells, CD19⁺ B cells, and CD49b⁺ NK cells, NK T cells, M1 and M2 macrophages, neutrophil, monocyte, cDC, pDC, and DC-P4 in the spleen (Supplementary Fig. 3A and 3B) and lymph nodes (Supplementary Fig. 3C and 3D) between wild-type and *DRG2*^{-/-} mice. In addition, DRG2 deficiency did not alter the differentiation of T cells because the frequency and number of CD4⁺CD8⁺, CD4⁺CD8⁻, and CD4⁻CD8⁺ T cells in thymus were similar in wild-type and *DRG2*^{-/-} mice infected with *L. monocytogenes* (Supplementary Fig. 3E and 3F). Consistently flow cytometry analysis of different subsets of immune cells showed no significant difference in the numbers and frequencies of CD4⁺, CD8⁺ T cells, CD19⁺ B cells, and CD49b⁺ NK cells, NK T cells, M1 and M2 macrophages, neutrophil, monocyte, cDC, pDC, and DC-P4 in the spleen (Supplementary Fig. 4A and 4B), lymph nodes (Supplementary Fig. 4C and 4D), and thymus (Supplementary Fig. 4E and 4F) between wild-type and *DRG2*^{-/-} mice *i.p.* infected with *L. monocytogenes*. These results suggest that DRG2 deficiency does not affect populations of immune cells in lymphoid organs.

Dexamethasone-induced reduction of inflammatory cytokines was independent of DRG2

Glucocorticoid hormones display potent immunosuppressive and anti-inflammatory activity (41), and therefore synthetic glucocorticoids (GC), such as dexamethasone (Dex), have been found to be particularly useful in the treatment of various inflammatory diseases (41). The anti-inflammatory actions of GC affect many cell types through a receptor-mediated process, and include profound effects on leucocyte distribution that are mediated in part by inhibition of production and release of many proinflammatory mediators, including cytokines (42).

The generally accepted view of anti-inflammatory actions on macrophages is through the suppression of NF- κ B activity, thus inhibiting the transcription of proinflammatory genes (43, 44).

Macrophages are resident phagocytic cells found in lymphoid and non-lymphoid tissues. Macrophages are critical effectors involved in steady-state tissue homeostasis, via the clearance of apoptotic cells, production of growth factors, and regulation of inflammation and the innate immune response. Macrophages are the first line of defense against microorganisms, which is accomplished by phagocytosis and the production of inflammatory cytokines (45).

After an immune response is induced by an external pathogen, cortisol, which reduces the immune response, is secreted in the body to maintain homeostasis. We investigated whether the reason for the decreased serum inflammatory cytokines in DRG2^{-/-} mice is affected by cortisol. In BMM of WT and DRG2^{-/-}, pretreated with dexamethasone and treated with LPS and *L. monocytogenes*, it was checked whether the induction of cytokine expression was reduced (Fig. 3A, 3B, 3C, 3D and 3F). From the results, it could be confirmed that the expression of IL-6 was drastically decreased after dexamethasone treatment, but this decrease occurred irrespective of DRG2. In addition, the secretion of cortisol from the body is a hormone that reduces the excessively increased immune response after removing external pathogens. To confirm the body-like state, IL-6 was induced by treatment with LPS and *Listeria* first, and then dexamethasone was treated (Fig. 3G and 3H). Consistent with the results of dexamethasone pretreatment, it was confirmed that the decrease in IL-6 was decreased in both WT and DRG2^{-/-} BMDM. From these results, it was confirmed that the decreased level of IL-6 in DRG2^{-/-} macrophage compared to WT after stimulation was not related to the decrease in inflammation caused by cortisol.

DRG2 deficiency inhibits NF-κB pathway

TNF- α , IL-6 and IL-1 β are target genes of NF- κ B (35, 36). We therefore tested whether the decrease in TNF- α , IL-6 and IL-1 β production in *DRG2*^{-/-} macrophages was caused by the decrease in NF- κ B activity. DRG2 deficiency was confirmed by Western blot analysis (Fig. 4A). To test this possibility, wild-type and *DRG2*^{-/-} BMDMs were stimulated in vitro with FSL-1 and ChIP was performed to analyze the p65 NF- κ B recruitment to TNF- α , IL-6 and IL-1 β promoter regions. As shown in Fig. 4B, in *DRG2*^{-/-} BMDMs, the recruitment of p65 NF- κ B to the promoters of TNF- α , IL-6 and IL-1 β was significantly inhibited compared with that of wild-type BMDMs. These results indicate that DRG2 deficiency suppresses the binding of NF- κ B to promoters of its target genes induced by *L. monocytogenes* stimulation in macrophages.

Recently, we found that DRG2 deficiency increased Akt activity and thus decreased GSK3 β activity in cancer cells (7). GSK3 β has been reported to phosphorylate NEMO (20), promote NF- κ B activity (37), and enhance NF- κ B-dependent proinflammatory cytokine expression (9). We thus tested whether DRG2 deficiency affect Akt and GSK3 β activity in BMDMs stimulated with FSL-1. Consistent with our previous result, *DRG2*^{-/-} BMDMs had significantly increased the levels of phosphorylated Akt and GSK3 β phosphorylated at serine 9 (inhibitory phosphorylation) after FSL-1 stimulation compared with wild-type BMDMs (Fig. 4C). In addition, we found that the levels of phosphorylated I κ B in *DRG2*^{-/-} BMDMs were significantly low compared with those in wild-type BMDMs (Fig. 4C). These results suggest that *DRG2*^{-/-} BMDMs have decreased GSK3 β activity and thus show defects in activation of NF- κ B after FSL-1 stimulation.

Upon activation, of NF- κ B is translocated from the cytoplasm into the nucleus where it induces the transcription of its target genes (21). We next tested whether DRG2 depletion affects the nuclear accumulation of NF- κ B. Wild-type and *DRG2*^{-/-} BMDMs were stimulated with FSL-1 and NF- κ B levels in the cytoplasmic and nuclear fractions were analyzed by western blotting. *DRG2*^{-/-} BMDMs showed a reduced nuclear localization of NF- κ B compared with wild-type BMDMs (Fig. 4D). To validate this, we determined the subcellular localization of NF- κ B by immunofluorescence microscopy. After FSL-1 stimulation, nuclear localization of

NF- κ B was significantly decreased in *DRG2*^{-/-} BMDMs (Fig. 4E, 4F). Collectively, our results suggest that DRG2 deficiency suppresses the NF- κ B activity in macrophages.

DRG2 deficiency delayed monocyte recruitment to the peritoneal cavity in *L. monocytogenes*-infected mice

Monocytes have important roles in early host defense responses against microbial pathogens. They develop in the bone marrow and egress into the circulation after infection (38). Before infection, monocytes in the bone marrow were similar (Fig. 5A, 5B), suggesting that DRG2 deficiency does not affect basal differentiation of monocytes in mice. After *i.p.* infection of *L. monocytogenes*, total cell counts of peritoneal monocytes markedly increased in both wild-type and *DRG2*^{-/-} mice (Fig. 5C, 5D). Even though number of monocytes in the peritoneal cavity of *L. monocytogenes*-infected *DRG2*^{-/-} mice was lower than that of wild-type mice until day 2 p.i., it reached to the similar level to that of wild-type mice at day 3 p.i., (Fig. 5C, 5D). The number of intraperitoneal neutrophils in *DRG2*^{-/-} mice infected with *L. monocytogenes* was also lower than in wild-type mice until 3 h p.i., but reached similar levels to wild-type mice at 6 h p.i. (Fig. 5E, 5F). We further investigated whether DRG2 deficiency affects the intrinsic migratory capacity of monocytes using in vitro transwell migration assay. The numbers of migrated *DRG2*^{-/-} monocytes were significantly low compared with WT cells until 6 h after incubation (Fig. 5G, 5H). However, at 22 h after incubation, similar number of migrated cells were observed in both wild-type and *DRG2*^{-/-} monocytes (Fig. 5H). Taken together, these results suggest that DRG2 deficiency delays the influx of monocytes to the peritoneal cavity during bacterial infections.

DRG2 deficiency does not affect the phagocytosis of *L. monocytogenes* by macrophages

To investigate whether DRG2 deficiency affects the phagocytosis of *L. monocytogenes*, we infected wild-type and *DRG2*^{-/-} macrophages with CFSE-labeled *L. monocytogenes* and cells were analyzed by flow cytometry. To quench

extracellular bacteria-derived fluorescence, trypan blue was used, as described (34). In the absence of trypan blue treatment, around 60% of both wild-type and *DRG2*^{-/-} macrophages had strong fluorescent signal, indicating that there was no difference in the numbers of *L. monocytogenes* associated with wild-type and *DRG2*^{-/-} macrophages (Supplementary Fig. 3A). After trypan blue treatment, about 30% of both wild-type and *DRG2*^{-/-} macrophages harbored intracellular *L. monocytogenes*. These results indicate that DRG2 deficiency does not affect the initial adherence of *L. monocytogenes* to macrophages and the internalization of bacteria. To verify our flow cytometry assay, we infected wild-type and *DRG2*^{-/-} macrophages with CFSE-labeled *L. monocytogenes* and, after trypan blue treatment, a minimum of 20 cells were counted under confocal microscope to quantify the percentage of cell population that contained internalized *L. monocytogenes*. Consistent with the flow cytometry assay, there was no difference in phagocytic efficiency between wild-type and *DRG2*^{-/-} macrophages (Supplementary Fig. 3B). We also determined whether DRG2 deficiency affects the bactericidal activity of macrophages. To test the hypothesis, we infected macrophages from wild-type and *DRG2*^{-/-} mice with *L. monocytogenes* and determined the growth of internalized bacteria using the gentamicin protection assay. We found that there was no significant difference in the growth of intracellular *L. monocytogenes* between these two groups (Supplementary Fig. 3C). Collectively, these results indicate that DRG2 is not required for the internalization of *L. monocytogenes* to macrophages and bactericidal activity of macrophages.

DRG2 deficiency increases sensitive to *L. monocytogenes* infection.

In the previous results, the function of macrophages in *DRG2*^{-/-} is significantly reduced. We thus hypothesized that DRG2 deficient mouse will be sensitive to *L. monocytogenes* infection. To test this hypothesis, wild-type (C57BL/6J) and *DRG2*^{-/-} mice were infected *i.p.* with *L. monocytogenes*. Since *DRG2*^{-/-} mice were slightly smaller than wild-type mice (wild-type, 22.3±0.7g; *DRG2*^{-/-}, 16.9±0.5g) (Supplementary Fig. 1), we compared the survival of mice infected with identical

bacterial doses per gram of body weight (5.5×10^4 CFU/g body weight, which equals 1.3×10^6 CFU and 1.0×10^6 per mouse in wild-type and *DRG2*^{-/-} mice, respectively) to exclude the bias by differences in body weight. We found that *DRG2*^{-/-} were more susceptible to *L. monocytogenes* infection than wild-type mice: all *L. monocytogenes*-infected *DRG2*^{-/-} mice died by day 7, while 50% of wild-type mice survived the infection and 30% of them were still alive at day 10 after infection. Kaplan-Meier analysis revealed a significant difference in survival between the two groups (Fig. 6A). Consistent with the mortality, while wild-type mice initially lost body weight (12% by day 4) and recovered to normal levels after day 5, *DRG2*^{-/-} mice underwent losing 20% of their initial body weight before succumbing to infection (Fig. 6B). To elucidate the underlying mechanisms of this increased susceptibility, we determined the bacterial loads in spleen and liver after infection. We first confirmed the DRG2 depletion in lymph node, thymus and spleen of *DRG2*^{-/-} mice by western blot (Supplementary Fig. 2). Consistent with survival data, significantly higher numbers of bacteria were counted in both liver (Fig. 6C) and spleen (Fig. 6D) of *DRG2*^{-/-} mice infected with *L. monocytogenes* than wild-type mice. Microabscess formation is a histological hallmark of *L. monocytogenes*-infected liver (39). To evaluate microabscess formation in the livers of *L. monocytogenes*-infected wild-type and *DRG2*^{-/-} mice, livers at day 3 post-infection were stained with H&E. Histopathology from *DRG2*^{-/-} mice showed significantly larger and more microabscesses than were seen in wild-type mice (Fig. 6E). To determine the role of DRG2 during alternative infection routes, wild-type and *DRG2*^{-/-} mice were intravenously (*i.v.*) infected with 1.5×10^5 c.f.u. of *L. monocytogenes*. Consistent with *i.p.*-infected mice, *DRG2*^{-/-} mice were more susceptible to *L. monocytogenes* infection than wild-type mice (Fig.

7A) and bacterial counts in the liver (Fig. 7B) and the blood (Fig. 7C) of *i.v.*-infected $DRG2^{-/-}$ mice were significantly higher than the burdens measured in wild-type mice at day 2 after infection. In addition, the microabscesses in $DRG2^{-/-}$ livers were significantly larger than those found in wild-type mice at day 2 after infection (Fig. 7D). These results suggest that $DRG2^{-/-}$ mice had defective innate immunity rendering them highly susceptible to *L. monocytogenes* infection.

Proinflammatory cytokine level following *L. monocytogenes* infection in WT and $DRG2^{-/-}$ mice varies with time point

We next analyzed proinflammatory cytokine levels in the sera and peritoneal fluids of wild-type and $DRG2^{-/-}$ mice *i.p.* infected with *L. monocytogenes*. We confirmed that macrophage and neutrophil migration were less in $DRG2^{-/-}$ mice in early time when listeria was infected in the peritoneal cavity (Fig. 5C, 5D, 5E, 5F). Therefore, *L. monocytogenes* was injected *i.p.* and proinflammatory cytokine levels in the peritoneal cavity and serum were checked at 1 hour. Consistent with the previous results, it was found that IL-6 levels were lower in $DRG2^{-/-}$ mice than in WT (Fig. 8A, 8B). TNF- α was not detected (Data was not shown). Since most of the infected $DRG2^{-/-}$ mice died by day 4 after *i.p.* infection, we analyzed inflammatory cytokines on day 3, when differences between wild-type and $DRG2^{-/-}$ mice should already be detectable. Unexpectedly, $DRG2^{-/-}$ mice produced significantly higher levels of serum TNF- α and IL-6 than wild-type mice (Fig. 8C and 8D). However, there was no significant difference in liver TNF- α and IL-6 levels between $DRG2^{-/-}$ and wild-type mice (Fig. 8E and 8F). We also analyzed the effect of $DRG2$

deficiency on the inflammatory cytokine production in mice *i.v.* infected with *L. monocytogenes*. Significantly high levels of TNF- α and IL-6 were detected from sera (Fig. 8G and 8H) and liver (Fig. 8I and 8J) of *i.v.*-infected *DRG2*^{-/-} mice compared with wild-type mice. These results suggest that proinflammatory cytokine level following *L. monocytogenes* infection in WT and *DRG2*^{-/-} mice varies with time point.

***DRG2*^{-/-} neutrophils shows defect in production of inflammatory cytokines**

Neutrophils as well as macrophages are cytokine-producing cells and play an important role in bacterial innate immunity (69). After infecting the *i.p.* and *i.v.* with *L. monocytogenes*, it was confirmed whether the late time increase in inflammatory cytokines was due to neutrophils. Bone marrow derived neutrophil (BMDN) was treated with *L. monocytogenes* and LPS. It was shown that the expression (Fig. 9A and 9B) and production (Fig. 9C and 9D) of IL6 in *DRG2* KO was lower than in WT. These results suggest that, like macrophages, *DRG2*^{-/-} neutrophils produced less amount of IL-6 after stimulation with *L. monocytogenes* or LPS.

***DRG2* depletion enhances the expression of inflammatory cytokines and chemokines in endothelial cells**

Endothelial cells have been shown to produce various cytokines and chemokines during inflammatory processes and may be a source of cytokines and chemokines during various infection (70). After infecting the *i.p.* and *i.v.* with *L. monocytogenes*, it was confirmed whether the late time increase in inflammatory cytokines was due

to endothelial cells. When mouse lung endothelial cells (mLEC) were treated with LPS, the expression of IL-6, IL-1 β , CXCL1 and CXCL2 in DRG2 KO was higher than in WT (Fig. 10A, 10B, 10C and 10D). These results suggest that, like macrophages, DRG2^{-/-} neutrophils produced less amount of IL-6 after stimulation with *L. monocytogenes* or LPS. These results suggest that the possibility that the late time increase in inflammatory cytokines after infecting the *i.p.* and *i.v.* with *L. monocytogenes* in mice is due to endothelial cells, unlike macrophages and neutrophils.

Macrophage DRG2 depletion leads to the susceptibility of *L. monocytogenes* infection.

To ascertain the role of the myeloid cell specific DRG2 deletion in infection with *L. monocytogenes*, we generated DRG2 macrophage specific KO mice. DRG2^{*fl/fl*} *LysM Cre*^{*+/-*} (DRG2 MKO) mice had normal appearance and body weight (Fig. S6) and showed no obvious behavioral abnormalities when compared to wild type, *LysM Cre* or DRG2^{*fl/fl*} mice. Their survival rate and fertility were normal in contrast to what has been reported in DRG2^{*-/-*} mice. Litter size and gender distribution were also normal. Western blot analysis of proteins from primary BMDM and peritoneal cell cultures showed robust DRG2 expression in DRG2^{*fl/fl*} mice and decreased DRG2 expression in DRG2 MKO mice (Fig. 11A). DRG2 protein reduced in DRG2 MKO male and female in primary BMDM and peritoneal cell in culture. DRG2^{*fl/fl*} and DRG2 MKO mice were infected *i.p.* with *L. monocytogenes*. We compared the survival of mice infected with identical bacterial doses per gram of body weight (5.5 x 10⁴ CFU/g body weight). We found that DRG2 MKO were more susceptible to *L. monocytogenes* infection than DRG2^{*fl/fl*}. Only 38% of *L. monocytogenes* infected DRG2 MKO mice survived by day 6, while 90% of DRG2^{*fl/fl*} mice survived the

infection and 60% of them were still alive at day 12 after infection. Kaplan-Meier analysis revealed a significant difference in survival between the two groups (Fig. 11B). Consistent with mortality, the loss in body weight between *DRG2^{fl/fl}* and MKO was significantly different (Fig. 11C). We determined the bacterial loads in spleen and liver after infection. The bacterial counts in the liver (Fig. 11D) of *i.p.*-infected *DRG2* MKO mice were significantly higher than the burdens measured in *DRG2^{fl/fl}* mice at day 3 after infection but not in the spleen (Fig. 11E). These results suggest that *DRG2* MKO had defective innate immunity rendering them highly susceptible to *L. monocytogenes* infection.

Macrophage depletion with Clodrolip dramatically increases sensitivity to *L. monocytogenes*

To study the function of macrophages in mice, depletion experiments can be performed with liposomes loaded with clodronate. Clodronate is a small hydrophilic bisphosphonate molecule and when encapsulated in liposomes is internalized by professional phagocytes, including macrophages (71). Once internalized, lysosomal phospholipases cause the release of clodronate into the cell and results in macrophage “suicide” or apoptosis (72). Clodronate has low toxicity for non-phagocytic cells, as it cannot easily escape the liposomal phospholipid bilayer (40). To test whether clodrolip can specifically deplete macrophages, PBS-liposome and clodrolip were injected *i.p.* into mice. Clodrolip was highly effective in reducing macrophages in spleen at 1 day after injection. The number of macrophages in spleen was reduced by 80% compared to mice receiving PBS-liposomes at the same time (Fig. 12A). To test the toxicity of clodrolip, the same amount as used for macrophage depletion was injected *i.p.* with clodrolip. All mice survived (Fig. 12B), and it was found that the weight was reduced by about 2% and then recovered. (Fig. 12C). From these results, it was confirmed that mice did not die only by injection of clodrolip. Mice were treated *i.p.* with PBS-liposome and clodronate liposomes to induce macrophage depletion. One day later, the mice were challenged *i.p.* with *L. monocytogenes*. To find out how macrophage depletion affects the defense against listeria, clodrolip was injected into WT and *DRG2^{-/-}* mice, and *L. monocytogenes*

was injected *i.p.* one day later. After macrophage depletion by treating WT with clodrolip, it was confirmed that all of mice injected with listeria died on the day 3 (Fig. 12D). We found that after depletion of macrophages by Clodrolip, both WT and DRG2 KO mice were equally sensitive to *L. monocytogenes* infection. These results suggest that macrophages are important in the initial immune response to *L. monocytogenes* and it showed that the decrease in the function of the *DRG2*^{-/-} macrophage can have a significant effect on the defense of *L. monocytogenes*.

Cells of γ -irradiated recipient mice determine the sensitivity to *L. monocytogenes* infection in bone marrow graft experiment

The ability to engraft mice with a hematopoietic system derived from another mouse provides the opportunity to study a variety of cell functions. Genetic disparities between donor and host owing to mutation, gene extinction, overexpression or selected insertions have provided models to unravel pathways of differentiation, function and even pathology (73). To further examine bone marrow cell responsible for DRG2-mediated dissemination of bacterial infections, we created WT and *DRG2*^{-/-} bone marrow chimeras. γ -irradiation kills bone marrow cells and is a condition for surviving tissue residential macrophages and stromal cells. *L. monocytogenes* was injected *i.p.* into the chimera, body weight, spleen weight, the number of bacteria in liver and spleen were confirmed (Fig. 12A, 12B, 12C and 12D). Bacterial load was not determined by DRG2 status in donor but by DRG2 status in recipient (Fig. 12D). These results suggest that the presence of DRG2 in residential macrophages plays an important role in susceptibility to *L. monocytogenes*.

Reconstitution of clodronate-treated mice with either macrophages from WT or *DRG2*^{-/-} mice does not protect mice from *L. monocytogenes* infection

To confirm that *DRG2*^{-/-} residential macrophage is important for sensitivity to *L. monocytogenes*, a macrophage graft using clodrolip was

performed. Macrophage depletion using Clodrolip can depletion both bone marrow macrophage and residential macrophage (Fig. 12A).

BMDM cells from WT and *DRG2*^{-/-} mice were injected into recipient mice depleted of both bone marrow macrophage and residential macrophage by injection of Clodrolip. Survival and body weight loss was confirmed by injecting *L. monocytogenes* into these mice (Fig. 14A, 14B) BMDM from both WT and *DRG2*^{-/-} donor mice did not protect both WT and *DRG2*^{-/-} recipient mice pretreated with Clodronate. These results suggest that depletion of DRG2 in residential macrophage is important for the sensitivity of *L. monocytogenes*.

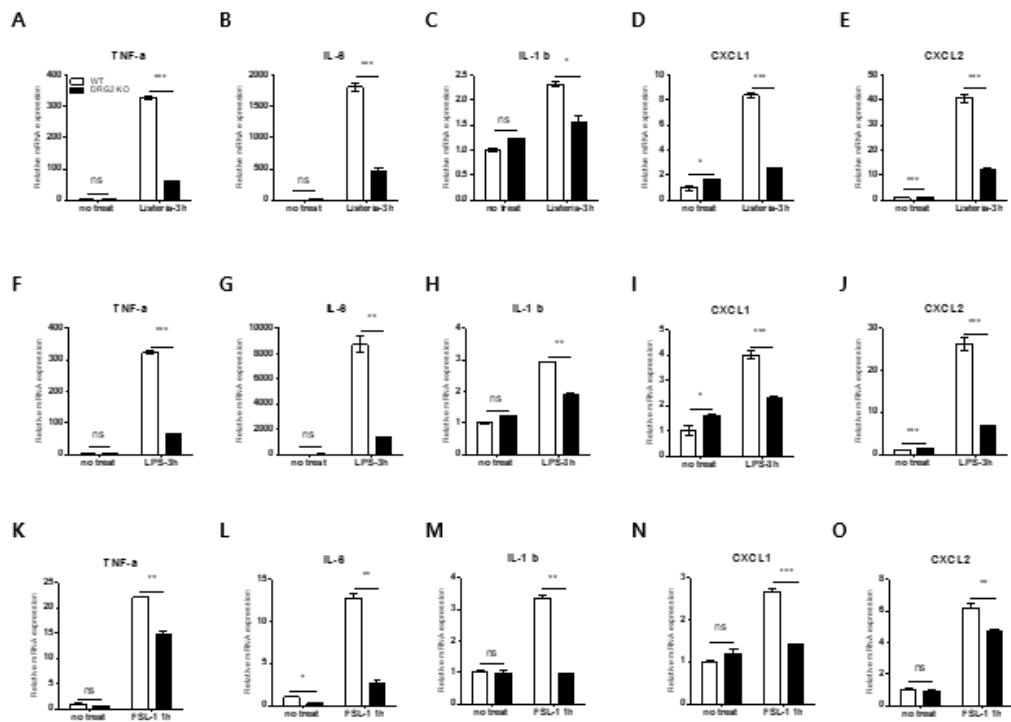


Figure 1. DRG2^{-/-} macrophages shows intrinsic defect in inflammatory cytokine and chemokine expression. (A-O) Bar graphs displaying cytokine and chemokine levels(qPCR) in WT and DRG2^{-/-} BMDMs (A-J) or peritoneal macrophages(K-O) stimulated with live *L. monocytogenes* (10MOI) (A-E), LPS (100ng/ml) (F-J) and FSL-1 (1ug/ml) (K-O) compared to controls. Data are mean \pm SEM (n = 2 or 3). * $p < 0.05$, ** $p < 0.01$, *** $p < 0.001$; ns, not significant

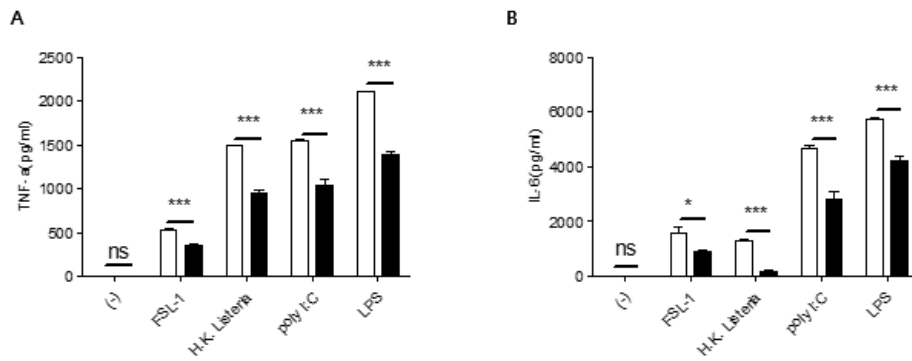


Figure 2. DRG2^{-/-} shows intrinsic defect in inflammatory cytokine production. (A-B) WT and DRG2^{-/-} peritoneal macrophages were exposed to FSL-1(1μg/ml), heat killed *L. monocytogenes*, poly I:C(20μg/ml), or LPS (1μg/ml) for 24 h and analyzed for (A) TNF-α and (B) IL-6 by ELISA. Data are mean ± SEM (n = 3). *p<0.05; **p<0.01; ***p<0.001.

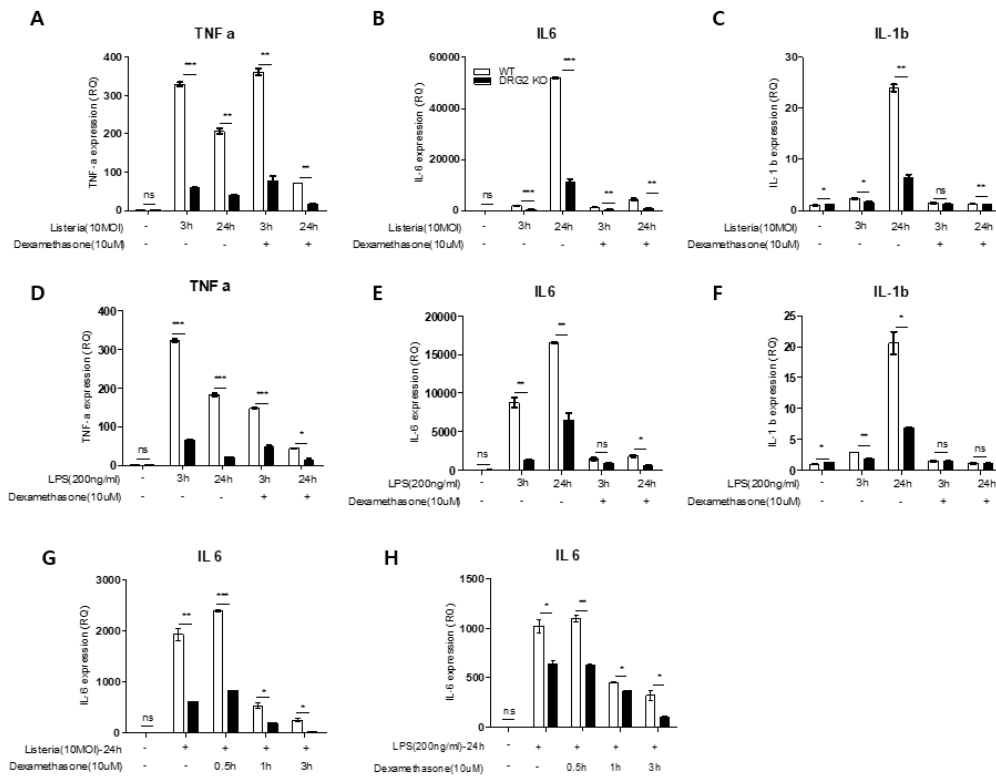


Figure 3. Dexamethasone-induced reduction of inflammatory cytokines was independent of DRG2. (A-C) WT and *DRG2*^{-/-} BMDM were exposed to *L. monocytogenes*(10MOI) and (D-F) LPS (200ng/ml) for indicated time point and analyzed for (A, D) TNF- α , (B, E, G, H) IL-6, (C, F) IL-1 β levels by qPCR. (A-F) Macrophages were pre-treated with dexamethasone 30 minutes before and then treated with LPS or *L. monocytogenes*. Macrophages were treated with *L. monocytogenes* or LPS and 24 hours later, treated with dexamethasone for the indicated time. Data are mean \pm SEM (n = 3). *p<0.05; **p<0.01; ***p<0.001.

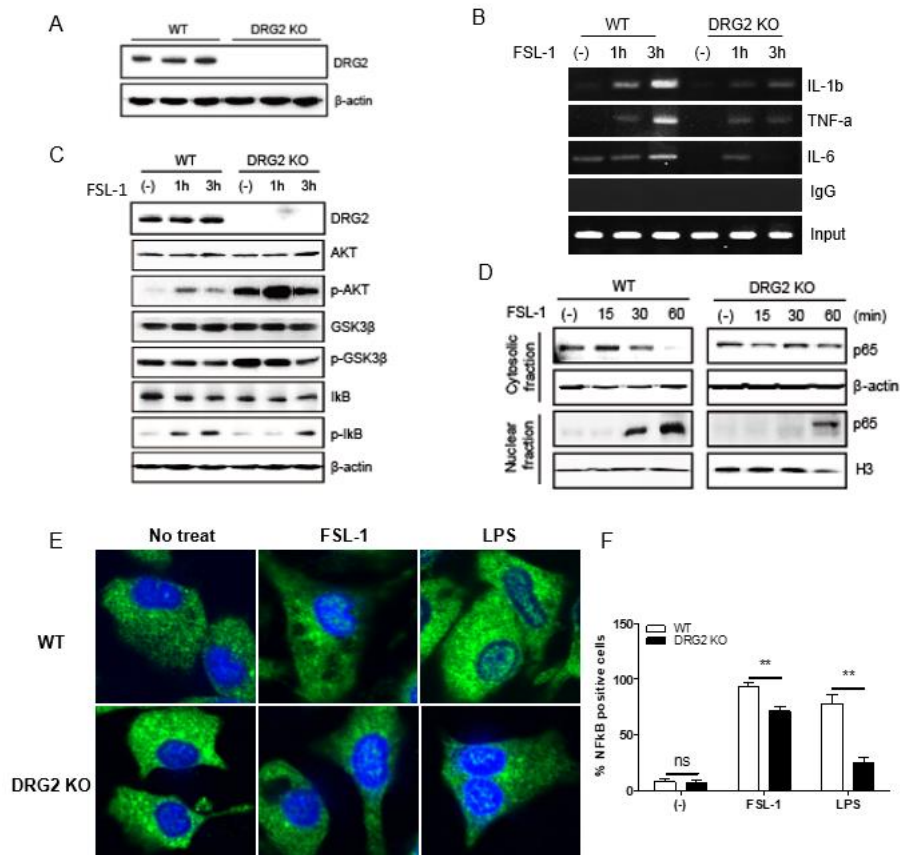


Figure 4. *DRG2*^{-/-} macrophages shows intrinsic defect in NF-κB activation pathway and inflammatory cytokine production. (A) Western blot analysis for DRG2 expression in BMDMs from wild-type and *DRG2*^{-/-} mice. (B) Chromatin immunoprecipitation (ChIP) analysis. WT and *DRG2*^{-/-} BMDMs were exposed to FSL-1 for indicated times. Formaldehyde cross-linked chromatin from cells was incubated with anti-p65 antibody. For negative controls, the chromatin was incubated with nonspecific IgG. Total input DNA at a 1/10 dilution was used as positive control for the PCR reaction. Immunoprecipitated DNA was analyzed by PCR with primers specific for the promoter of IL-1β, TNF-α or IL-6. (C-F) *DRG2* deficiency inhibits activity of GSK3β and NF-κB. WT and *DRG2*^{-/-} BMDMs were exposed to FSL-1 for indicated times. (C) Cell lysates were examined for phosphorylation of Akt, GSK3β, and IκB by western blot analysis. (D) NF-κB in the cytoplasmic and nuclear fractions was analyzed by Western blotting with

antibody against NF- κ B subunits p65. Histone and β -actin were used as internal markers for nuclear and cytoplasmic proteins. (E) Cells were fixed and stained anti- NF- κ B p65 antibody. Nuclei were stained with DAPI (blue). Representative confocal images are shown. Graph indicates the percent of cells with nuclear NF- κ B. Fifty cells were counted for each sample in triplicates. ** $p < 0.01$. ns, not significant

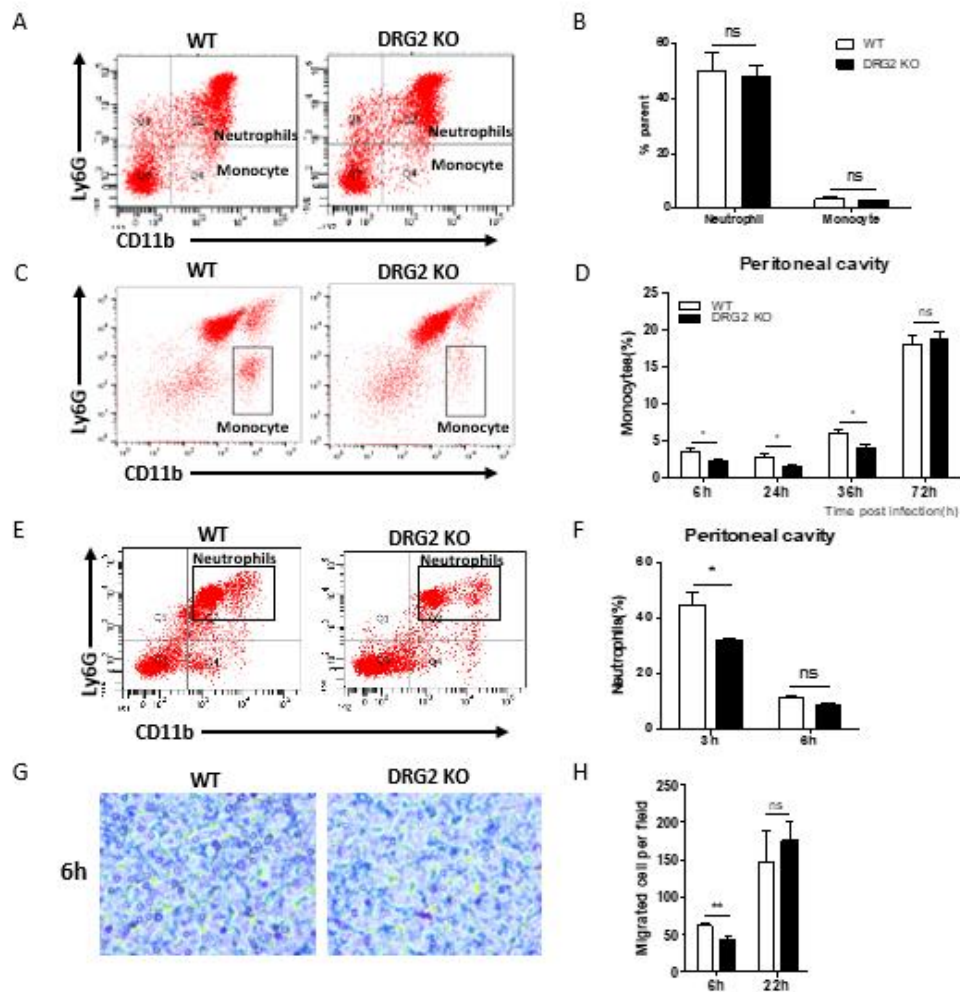


Figure 5. DRG2 deficiency attenuates the migration of monocytes and macrophages. (A) FACS analysis of CD11b⁺Gr-1⁺Ly6G^{low} monocytes in bone marrow of naïve wild-type and *DRG2*^{-/-} mice. (B) At indicated times after *L. monocytogenes* infection, peritoneal lavage was performed on wild-type and *DRG2*^{-/-} mice and cells collected were FACS analyzed for CD11b⁺Gr-1⁺Ly6G^{low} monocytes. (C) Peritoneal macrophages were collected from wild-type and *DRG2*^{-/-} mice and the migration of the macrophages were determined by the transwell chamber assay. Data are representative of three experiments. Data are presented as the mean ± SD (n = 3) (**p*<0.05; ***p*<0.01). ns, not significant. (D-F) DRG2 deficiency does not affect bacterial uptake and killing by macrophages. (D and E) Wild-type and *DRG2*^{-/-} macrophages were infected with CFSE-labelled

L. monocytogenes at 10 MOI for 1 h. (D) Cells were analyzed by flow cytometry in the absence of trypan blue. Values are means \pm SD (n = 3). (E) Cells were observed using confocal microscope in the presence of trypan blue (final concentration of 0.2%). Representative confocal images are shown. Graph indicates the number of bacteria per cell. Twenty cells were counted for each sample in triplicates. ns, not significant. (F) Intracellular growth of *L. monocytogenes* in wild-type and *DRG2*^{-/-} macrophages. Macrophages were infected with *L. monocytogenes* at an MOI of 5. Gentamicin was added 1 h *p.i.* to kill extracellular bacteria and bacterial growth was determined over a period of 8 h post infection (*p.i.*). The amounts of intracellular bacteria were enumerated. Each experiment was done three times in triplicate. Data are presented as the mean \pm SD (n = 3).

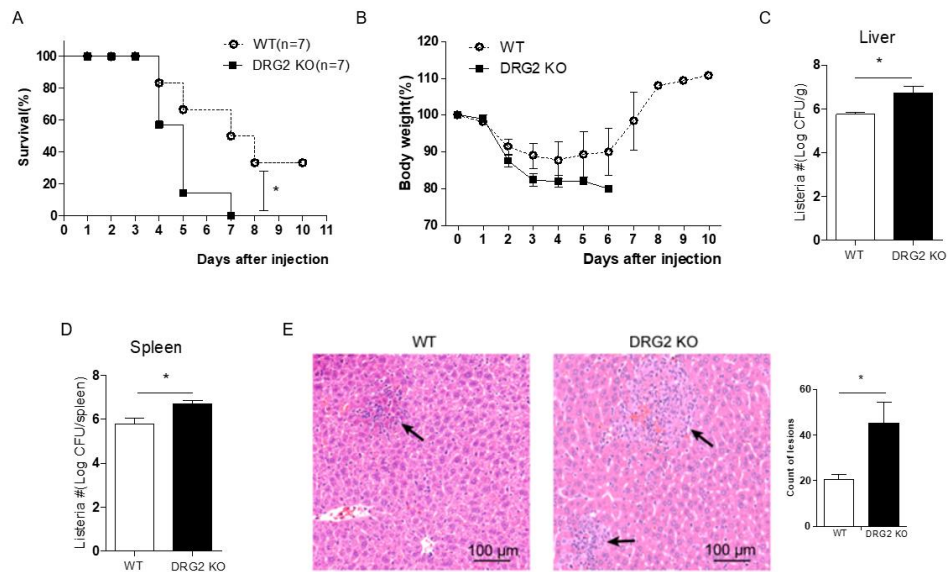


Figure 6. DRG2^{-/-} mice are sensitive to *i.p.* infection with *L. monocytogenes*. Wild-type (WT) and DRG2^{-/-} mice (7-week-old) were infected *i.p.* with 5.5 x 10⁴ *L. monocytogenes* per g of mouse body weight. (A) Survival and (B) proportion of weight loss was monitored daily for 10 days. The data are pooled from two independent experiments (n = 7 for WT and DRG2^{-/-} mice). Bacterial load in the liver (C) and spleen (D) was determined at 3 days p.i. (E) The large lobe of the liver was collected at 3 days p.i. and embedded in paraffin. Sections are stained with hematoxylin/eosin and representative of at least three mice per group. The liver microabscess was quantitated from H&E images and is presented as mean ± SEM. *p < 0.05; **p < 0.01

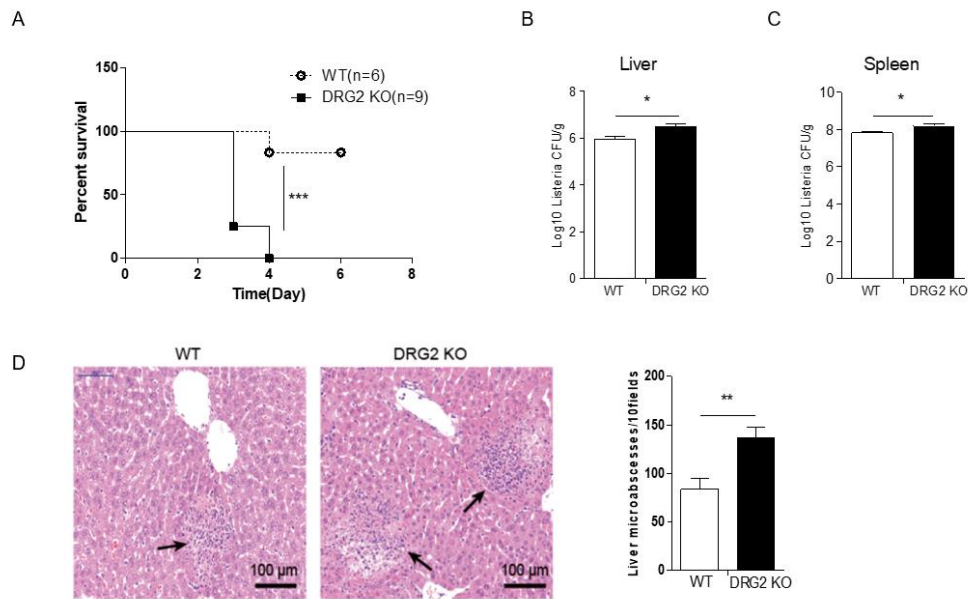


Figure 7. *DRG2*^{-/-} mice are sensitive to *i.v.* infection with *L. monocytogenes*. Wild-type (WT) and *DRG2*^{-/-} mice (7-week-old) were infected *i.v.* with 9.0×10^3 *L. monocytogenes* per g of mouse body weight. (A) Survival was monitored daily for 6 days. The data are pooled from two independent experiments (n = 7 for WT and *DRG2*^{-/-} mice). Bacterial load in the spleen (B) and blood (C) was determined at 2 days p.i. (D) The large lobe of the liver was collected at 2 days p.i. and embedded in paraffin. Sections are stained with hematoxylin/eosin and representative of at least three mice per group. The liver microabscess was quantitated from H&E images and is presented as mean \pm SEM. *p < 0.05; **p < 0.01.

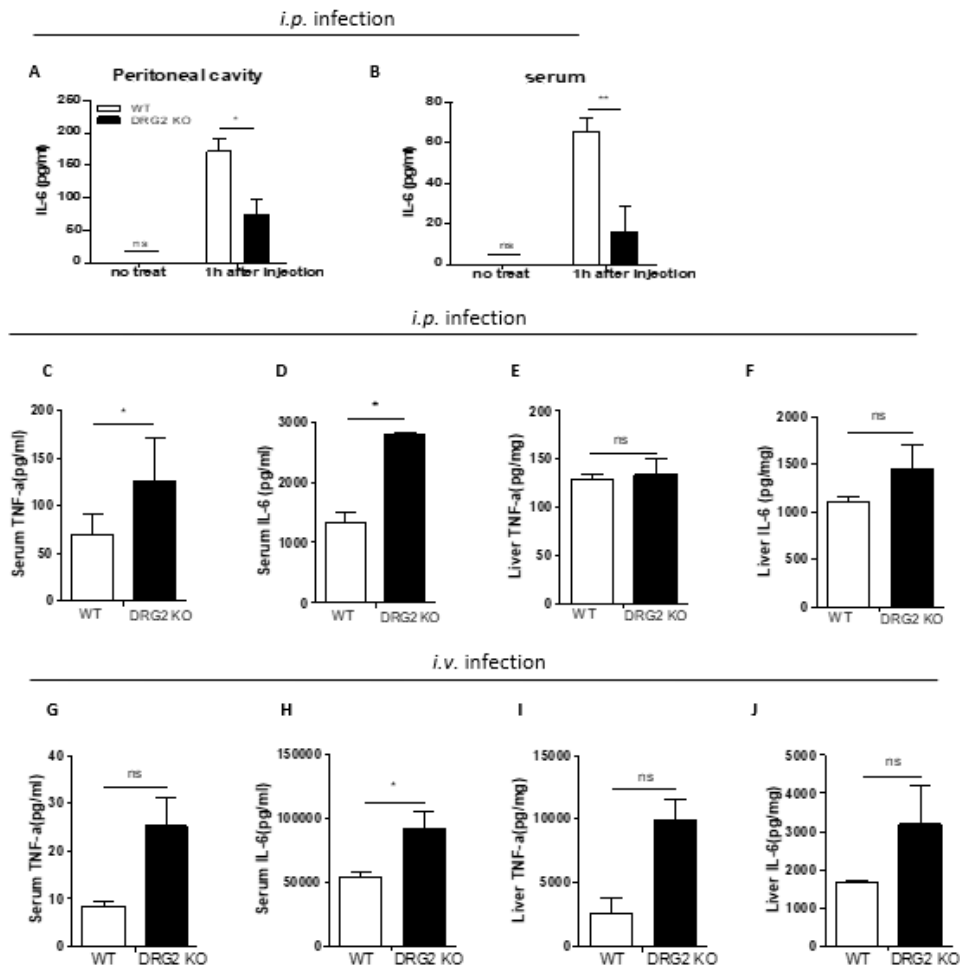


Figure 8. Cytokine production following *L. monocytogenes* infection in WT and *DRG2*^{-/-} mice. WT and *DRG2*^{-/-} mice were infected (A-D) *i.p.* with 5.5 x 10⁴ or (E-H) *i.v.* with 9.0 x 10³ *L. monocytogenes* per g of mouse body weight. Serum (A, B, E, F) and liver lysate (C, D, G, H) were collected from WT and *DRG2*^{-/-} mice at 2 days *p.i.* and analyzed for TNF- α and IL-6 by ELISA. (I-J) *i.p.* with 5.5 x 10⁴ *L. monocytogenes* per g of mouse body weight. Peritoneal lavage (I) and serum (J) were collected from WT and *DRG2*^{-/-} mice at 1 hour *p.i.* and analyzed for TNF- α (not detected, data not shown) and IL-6 by ELISA. Data are mean \pm SEM (n = 8–11 mice/group). *p < 0.05. ns, not significant.

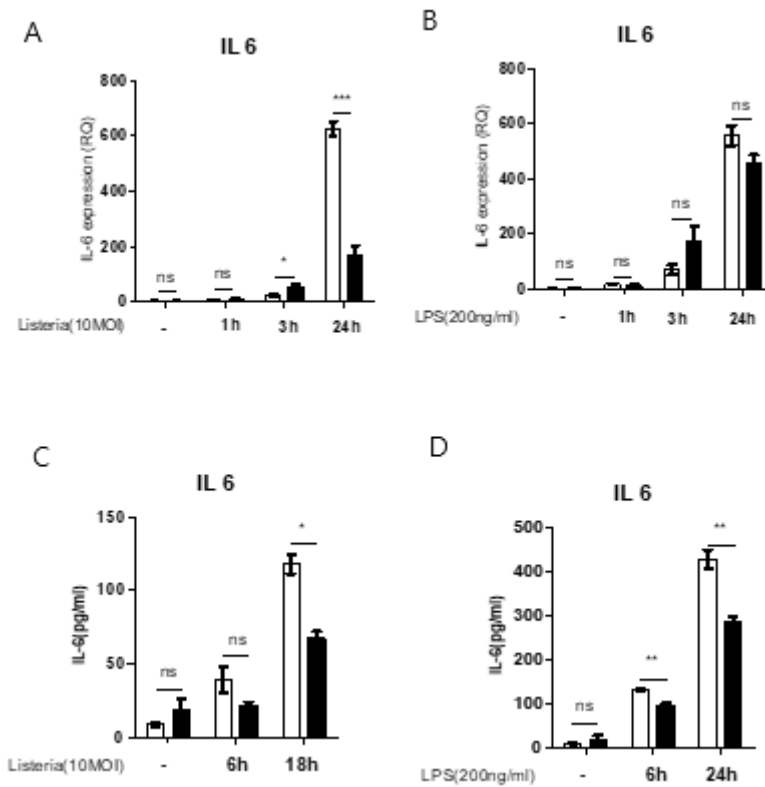


Figure 9. *DRG2*^{-/-} neutrophils shows defect in production of inflammatory cytokines. (A, B) Bar graphs displaying IL-6 expression levels by qPCR and IL-6 production by ELISA in WT and *DRG2*^{-/-} BMDNs stimulated with live *L. monocytogenes* (10MOI) (A, C), LPS (200ng/ml) (B, D) compared to controls. Data are mean \pm SEM (n = 2 or 3). * $p < 0.05$, ** $p < 0.01$, *** $p < 0.001$; ns, not significant.

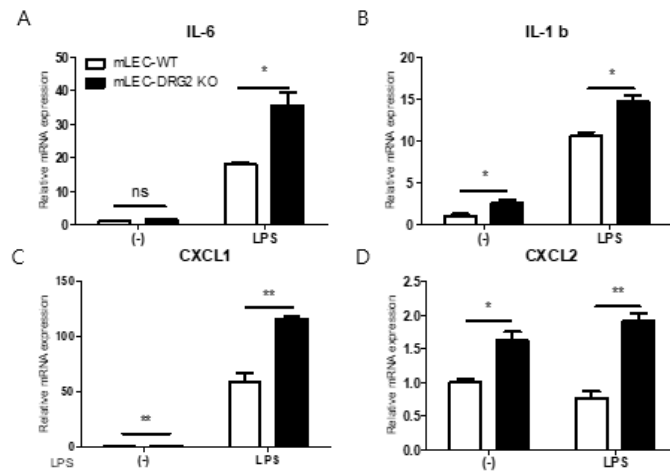


Figure 10. *DRG2* depletion enhances the expression of inflammatory cytokines and chemokines in endothelial cells. (A-D) Bar graphs displaying cytokine and chemokine levels by qPCR in WT and *DRG2*^{-/-} mouse lung endothelial cells (mLEC) stimulated with LPS (100ng/ml) for 3h compared to controls. Data are mean ± SEM (n = 2 or 3). **p*<0.05, ***p*<0.01, ns, not significant

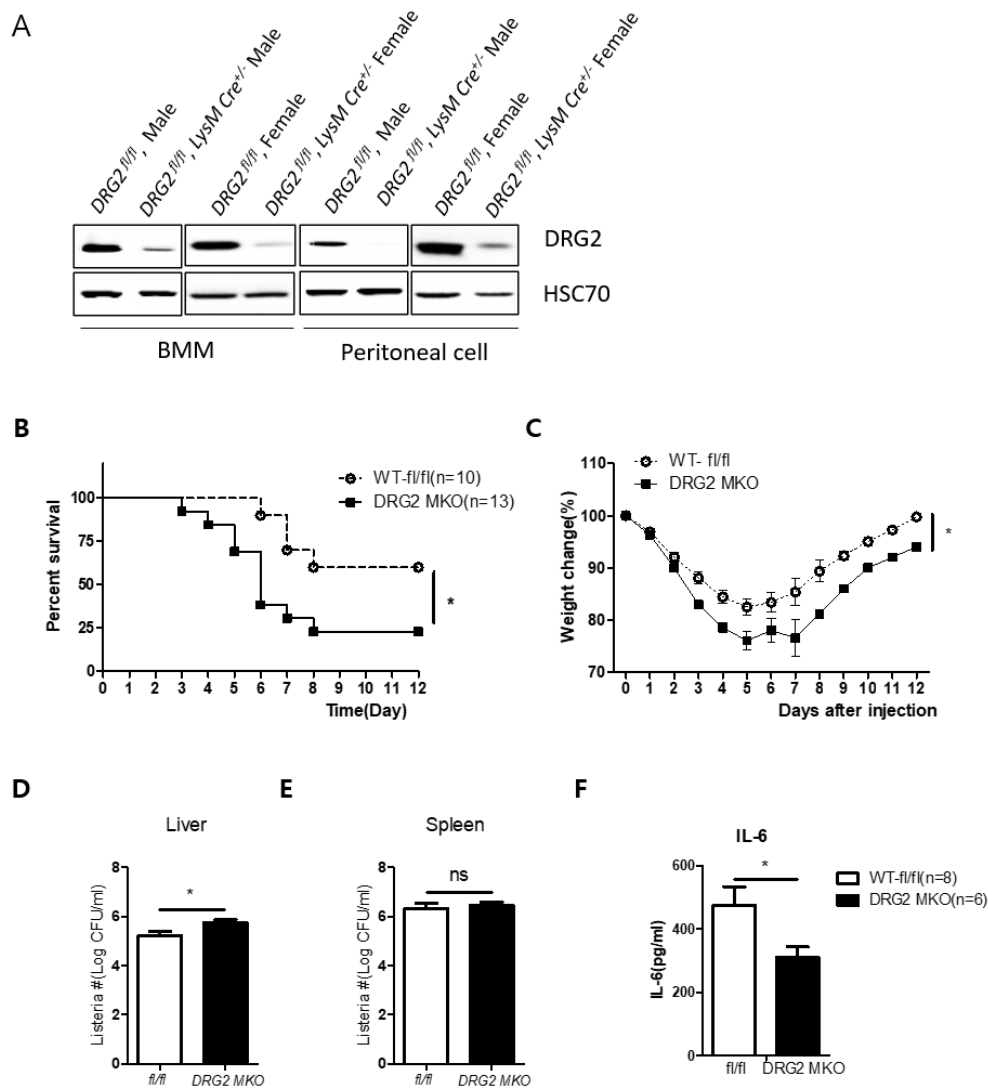


Figure 11. DRG2 MKO mice are sensitive to *i.p.* infection with *L. monocytogenes*. (A) BMM and peritoneal macrophages from both WT and DRG2 MKO mice were isolated and Western blot analysis for DRG2 was performed. The picture shows a representative Western Blot from peritoneal macrophages and each line represents one mouse. Wild-type (WT) and *DRG2*^{-/-} mice (8-week-old) were infected *i.p.* with 5.5×10^4 *L. monocytogenes* per g of mouse body weight. (A) Survival and (B) proportion of weight loss was monitored daily for 12 days. The data

are pooled from three independent experiments (n = 10~13) for WT and DRG2^{-/-} mice. Bacterial load in the liver (D) and spleen (E) was determined at 3 days *p.i.* *p < 0.05, *ns*, *not significant*.

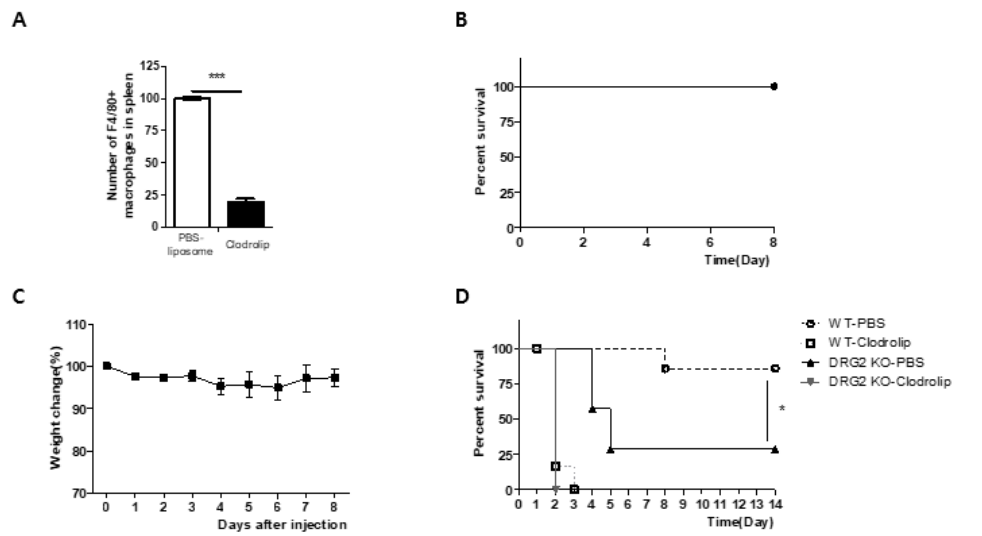


Figure 12. Macrophage depletion with Clodrolip dramatically increases sensitivity to *L. monocytogenes*. (A) FACS analysis of macrophages in spleen 1 day after *i.p.* injection with PBS-liposome and clodrolip. Wild-type (WT) mice (8-week-old) were infected *i.p.* with clodrolip of mouse body weight(1mg/20g). (B) Survival and (C) proportion of weight loss was monitored daily for 8 days. (D) Wild-type (WT) and *DRG2*^{-/-} mice (8-week-old, male) were injected *i.p.* with PBS-liposome and clodrolip of mouse body weight(1mg/20g). After 1 day wild-type (WT) and *DRG2*^{-/-} mice were infected *i.p.* with 5.5×10^4 *L. monocytogenes* per g of mouse body weight. Survival was monitored daily for 14 days.

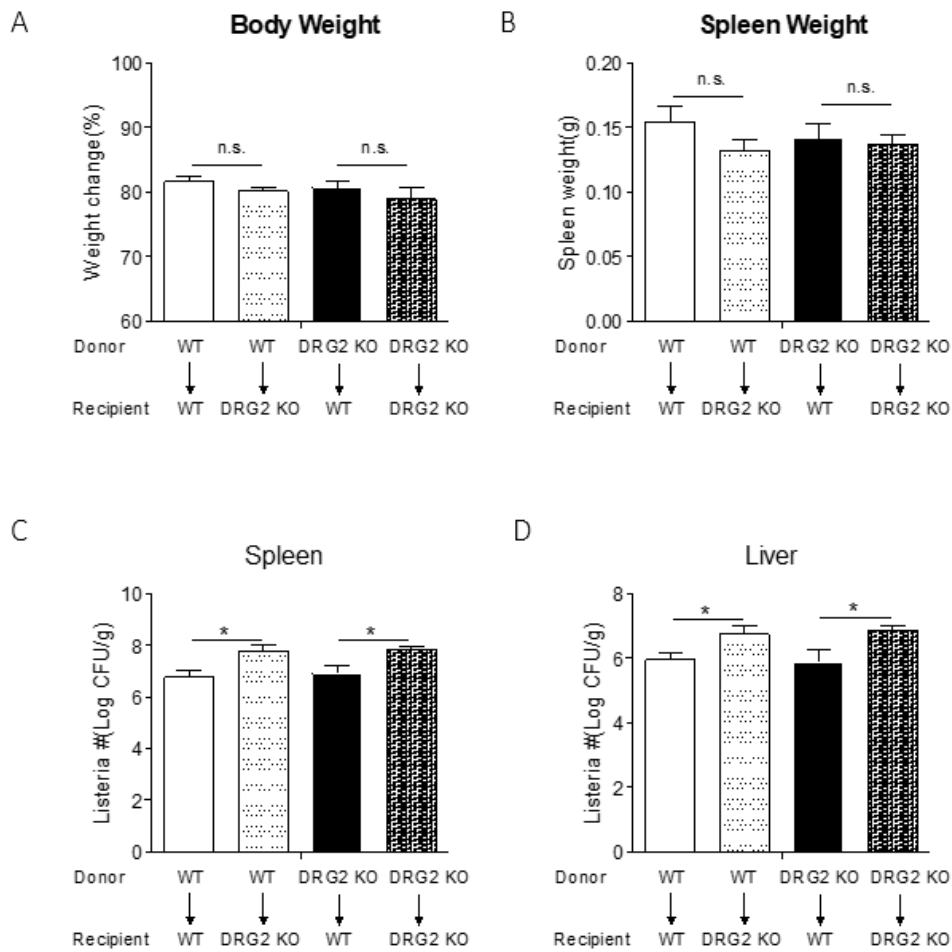


Figure 13. Cells of γ -irradiated recipient mice determine the sensitivity to *L. monocytogenes* infection in bone marrow graft experiment. (A-D) Bone-marrow chimera mice were generated for *DRG2* as described in methods. Bar graph shows the percent of weight loss(A) and spleen weight(B) in four groups of chimeric mice. Different groups of chimeric mice, as indicated in the figure panels, were infected with *L. monocytogenes* and bacterial loads were determined in the liver(C) and spleen(D) on day 3. Data show mean \pm s.e.m. of a representative experiment.

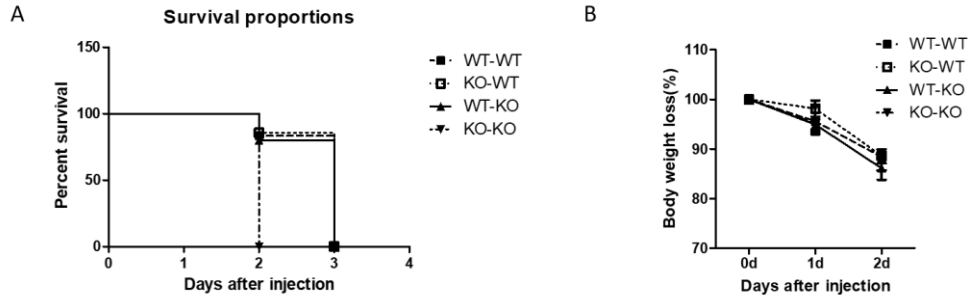
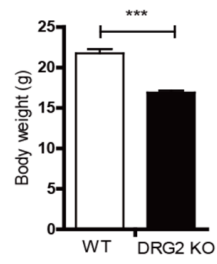
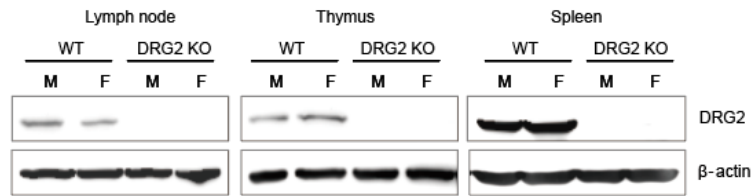


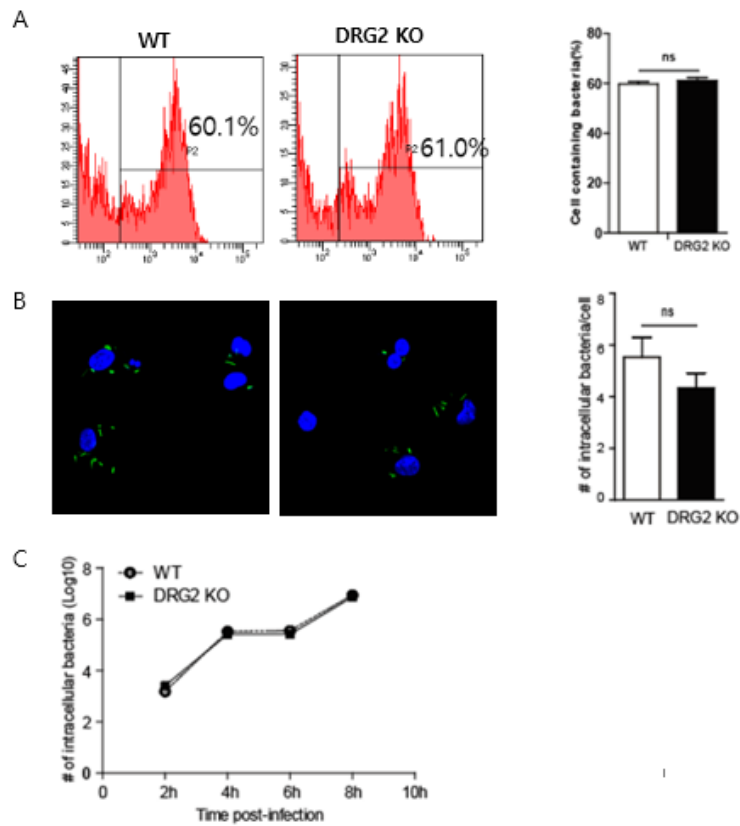
Figure 14. Reconstitution of Clodronate-treated mice with either macrophages from WT or DRG2 KO mice does not protect mice from *L. monocytogenes* infection. (A-B) Clodrolip depletion and BMDM reconstitution mice were generated as described in methods. Bar graph shows the percent of weight loss(A) and body weight loss(B) in four groups of grafted mice. Different groups of grafted mice, as indicated in the figure legends, were infected with *L. monocytogenes*.



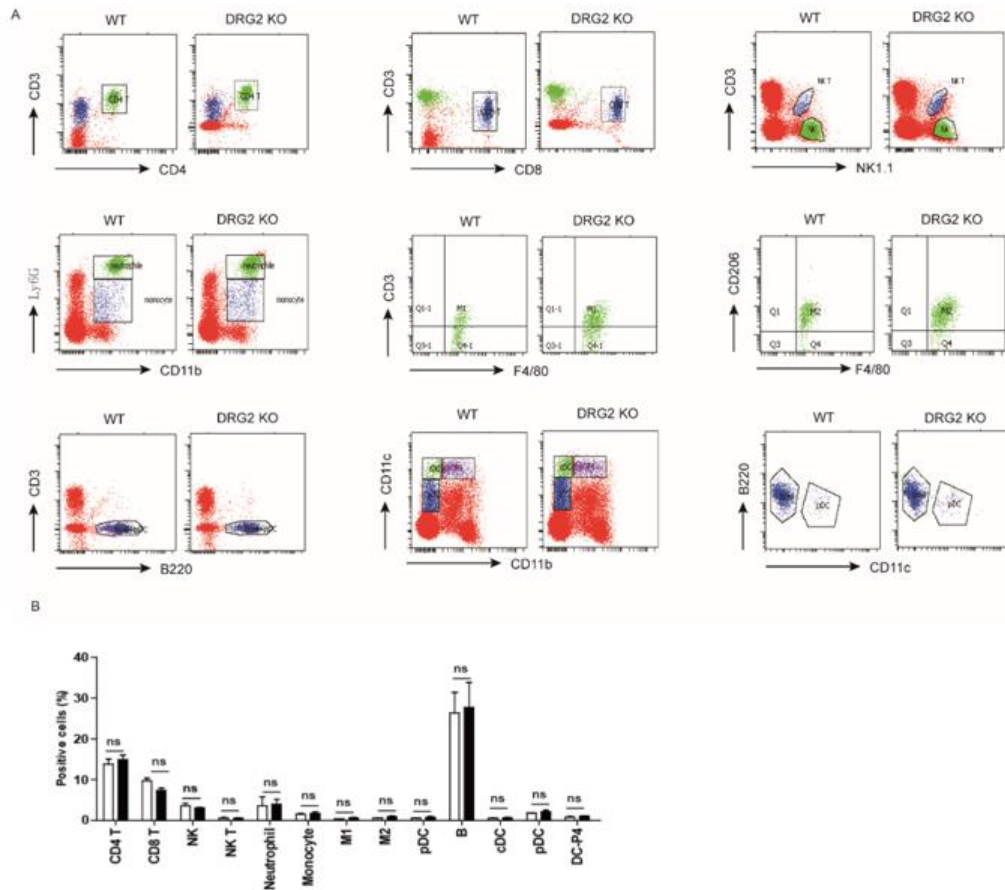
Supplementary Figure S1. Body weight of wild-type and DRG2^{-/-} mice. The body weight of 7-week-old mice (n=7) is presented as mean \pm S.D. *p < 0.05.



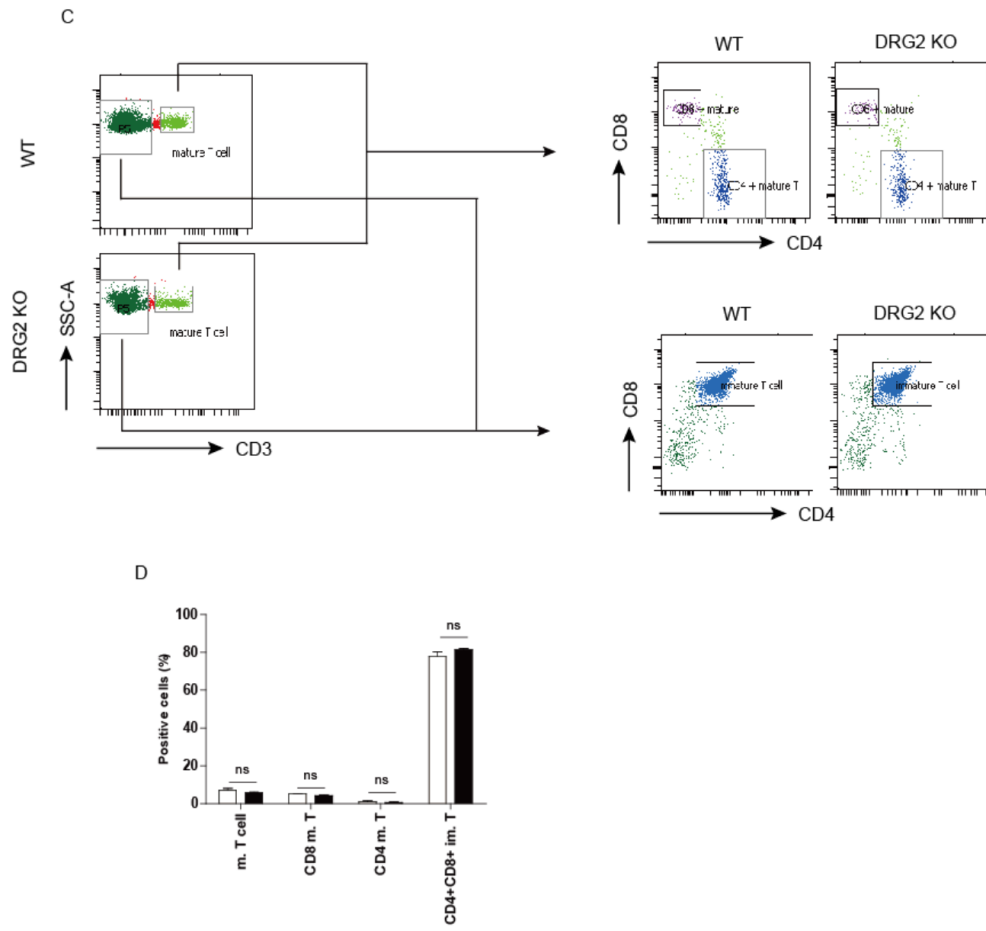
Supplementary Fig.S2. Western blot analysis for the expression of DRG2 protein in lymph node, thymus, and spleen of wild-type and DRG2^{-/-} mice. M; male, F; female.



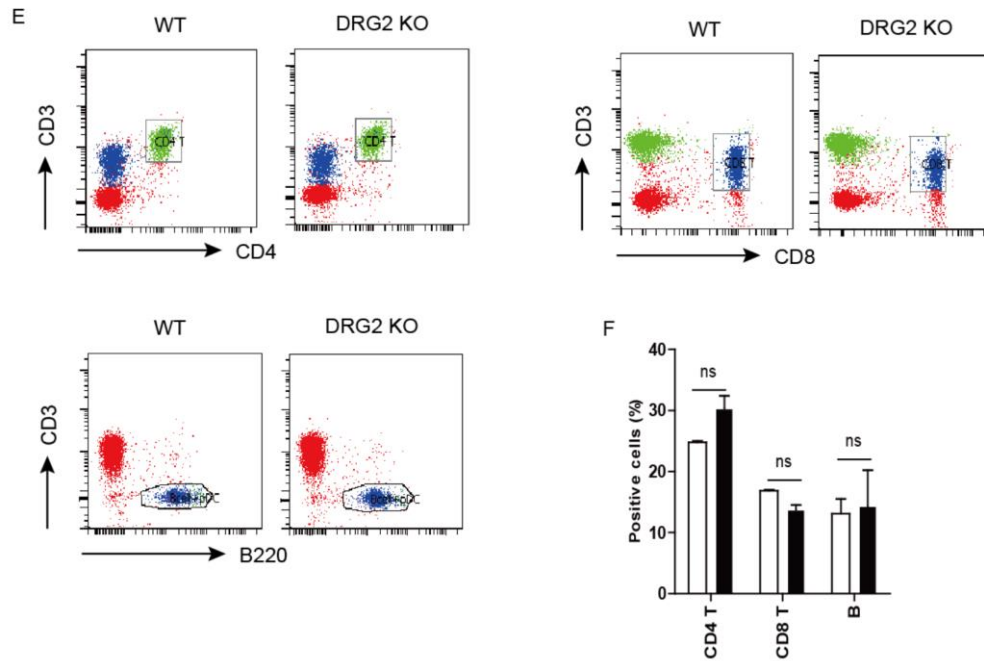
Supplementary Fig.S3. DRG2 deficiency does not affect the uptake and killing of bacteria by macrophages. (A) Cells were analyzed by flow cytometry in the absence of trypan blue. Values are means \pm SD ($n = 3$). (B) Cells were observed using confocal microscope in the presence of trypan blue (final concentration of 0.2%). Representative confocal images are shown. Graph indicates the number of bacteria per cell. Twenty cells were counted for each sample in triplicates. ns, not significant. (C) Intracellular growth of *L. monocytogenes* in wild-type and *DRG2*^{-/-} macrophages. Macrophages were infected with *L. monocytogenes* at an MOI of 10. Gentamicin was added 1h p.i. to kill extracellular bacteria and bacterial growth was determined over a period of 8 h post infection (p.i.). The amounts of intracellular bacteria were enumerated. Each experiment was done three times in triplicate. Data are presented as the mean \pm SD ($n = 3$).



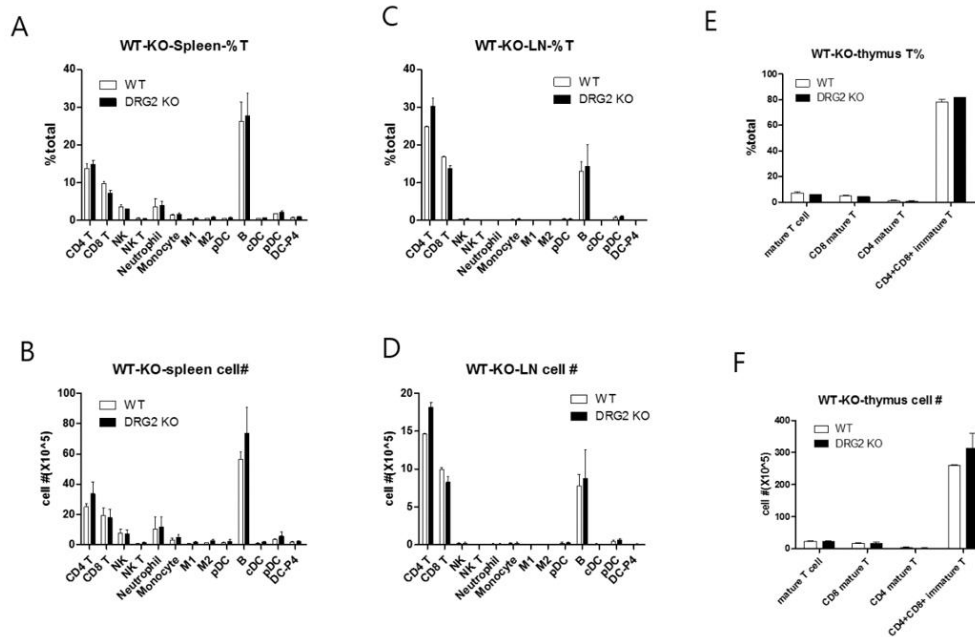
Supplementary Fig.S4.



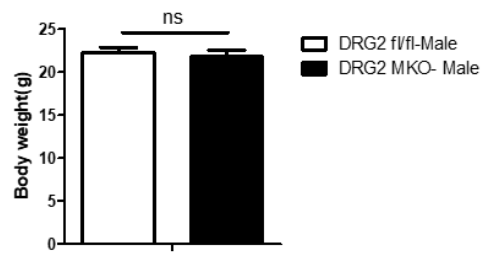
Supplementary Fig.S4.



Supplementary Fig.S4. DRG2 deficiency does not affect the popularities of immune cells in lymphoid organs. FACS analysis of immune cell subsets in lymphoid organs of WT and *DRG2*^{-/-}. Cells were collected from (A and B) spleen, (C and D) lymph nodes, and (E and F) thymus of wild-type and *DRG2*^{-/-} mice. Cells were stained for CD3, CD4, CD8, B220, NK1.1, Ly6G(Gr-1), CD11b, F4/80, and CD197(CCR7). (B, D, F) Bar graphs represent percentage of indicated populations. Values are means ± SD (n = 3).



Supplementary Fig. S5. DRG2 deficiency does not affect the popularities of immune cells in lymphoid organs. FACS analysis of immune cell subsets in lymphoid organs of WT and DRG2^{-/-} mice *i.p.* infected with *L. monocytogenes*. Cells were collected from (A and B) spleen, (C and D) lymph nodes, and (E and F) thymus of wild-type and DRG2^{-/-} mice at 48 h after *L. monocytogenes* infection. Cells were stained for CD3, CD4, CD8, B220, NK1.1, Ly6G(Gr-1), CD11b, F4/80, and CD197(CCR7). (A, C, E) Bar graphs represent percentage of indicated populations. Values are means \pm SD (n = 3). (B, D, F) Bar graphs are quantifications of indicated populations. Values are means \pm SD (n = 3).



Supplementary Figure S6. Body weight of $DRG2^{fl/fl} LysM Cre^{-/-}$ and $DRG2^{fl/fl} LysM Cre^{+/-}$ mice. The body weight of 7-week-old mice (n=7) is presented as mean \pm S.D. *p < 0.05.

Discussion

Proinflammatory cytokines such as TNF- α , IL-1, IL-6, are essential for primary defense against infection with *L. monocytogenes* (46, 47, 48). IL-6 is a major inducer of acute phase proteins and is involved in the control of neutrophil and monocyte responses following infection. IL-6 is also a survival factor for lymphocytes and it promotes Ab production by B cells (49, 50, 51). Infection also leads to robust production of IL-6, and IL-6 deficiency or IL-6 neutralization with Abs results in enhanced susceptibility to *L. monocytogenes* (52, 53, 54, 55, 56); however, mechanisms of IL-6-mediated protection are so far unclear. Recently, IL-6 has been identified as a decisive cytokine for the differentiation of CD4⁺ T cells into Th17 cells, which are considered to be a major proinflammatory T cell population (57, 58). As a consequence, blockade of IL-6 or IL-6 signaling has a profound impact on innate and acquired immune responses. Impaired IL-6 function causes enhanced susceptibility of mice to infection with various pathogens (52, 59, 60, 61). Therefore, we suggest that a decrease in IL-6 produced by listeria in DRG2 KO mice increases susceptibility to *L. monocytogenes*.

The key question arising from our data was how DRG2 deficiency inhibits the production of proinflammatory cytokines in macrophages. NF- κ B plays a critical role in the inflammatory response against a Listeria infection (29, 30, 31). We previously reported that overexpression of DRG2 enhances PPAR γ activity and stabilizes binding of NCoR to NF- κ B binding site, which inhibits NF- κ B activity and IL-6 production from macrophages (5). In this study, we initially expected that DRG2^{-/-} macrophages would show enhanced NF- κ B activity and inflammatory cytokine production. However, contrary to our expectation, DRG2^{-/-} macrophages showed decrease in NF- κ B activity and inflammatory cytokine production. Recently we found that DRG2 depletion enhances Akt activity and inhibitory phosphorylation of GSK3 β in cancer cells (7). Consistently, we here demonstrated that DRG2^{-/-} macrophages show enhanced Akt activity and inhibitory phosphorylation of GSK3 β following *L. monocytogenes* stimulation. It has been reported that GSK3 β phosphorylates NEMO, promotes NF- κ B activity, and enhances NF- κ B-dependent proinflammatory cytokine expression (62, 16, 9). Thus, it is possible to predict that

enhanced inhibitory phosphorylation of GSK3 β in *DRG2*^{-/-} macrophages inhibits NF- κ B activity, leading to decrease in the production of proinflammatory cytokines after *L. monocytogenes* stimulation. We here provided supporting evidences: *DRG2*^{-/-} macrophages showed reduced nuclear accumulation and DNA binding activity of NF- κ B upon stimulation with *L. monocytogenes*. Although the exact mechanism(s) underlying the DRG2-mediated regulation of NF- κ B activity in macrophages remains unclear, our results suggest that *DRG2*^{-/-} deficiency inhibits GSK3 β activity, resulting in down-regulation of NF- κ B activity and proinflammatory cytokine production in macrophage.

Both innate and adaptive immunity are required for control of *L. monocytogenes* infection (63, 64, 65). Following infection with *L. monocytogenes*, while innate immune responses are rapidly triggered and protect animals from lethal infection (66 65), adaptive immunity mediated by T cells is required for final clearance of bacteria in a sub-lethal infection (63, 64). In this study, mice were lethally infected with *L. monocytogenes* and the infected animals began to die from day 4 after infection. We therefore hypothesized that defects in innate immunity might be a crucial factor for attenuated bacterial clearance in *DRG2*^{-/-} mice upon *L. monocytogenes* infection. Analysis of innate immune response of *DRG2*^{-/-} mice after *L. monocytogenes* infection revealed that the frequency and the number of Ly6C^{hi} monocytes in bone marrow of *DRG2*^{-/-} mice were comparable to those of wild-type mice. In addition, there was no difference in the binding of *L. monocytogenes* to macrophages and the survival of phagocytosed *L. monocytogenes* between *DRG2*^{-/-} and wild-type macrophages. These suggest that *DRG2*^{-/-} mice are not defective in monocyte generation in bone marrow and bacterial sensing and killing by macrophages. However, *DRG2*^{-/-} macrophages showed intrinsic defects in homing to the infection site and production of inflammatory cytokines and chemokines including TNF- α , IL-6 IL-1 β , CXCL1 and CXXL2. These suggest that these defects in macrophages functions may lead to attenuated bacterial clearance in *DRG2*^{-/-} mice upon *L. monocytogenes* infection.

To ascertain the role of the myeloid cell-specific DRG2 deletion in infection with *L. monocytogenes*, we generated DRG2 macrophage specific KO mice. Consistent

with the results in *DRG2*^{-/-} mice, myeloid DRG2 deletion leads to the susceptibility of *L. monocytogenes* infection. These results suggest that macrophage-specific DRG2 KO, which excludes the influence of other cells, also has a defective innate immunity that makes it highly susceptible to *L. monocytogenes* infection.

In summary, our findings reveal a novel mechanism by which DRG2 regulates innate immunity against *L. monocytogenes* infection. Our data suggest that DRG2 is required for activation of GSK3 β and NF- κ B in macrophages. *DRG2*^{-/-} macrophages showed defects in NF- κ B activation, pro-inflammatory cytokine production and bacterial clearance at early stage of *L. monocytogenes* infection. *DRG2*^{-/-} mice showed enhanced susceptibility against *L. monocytogenes* infection. Considering that innate immunity is essential for early defense against *L. monocytogenes* infection, our data suggest that DRG2 plays a role in host defense against *L. monocytogenes* infection. If DRG2-mediated regulation of innate immunity is also involved in the protection against *L. monocytogenes* infection in human, temporary induction of DRG2 expression or its activity might represent a promising target for therapeutic interventions.

References

1. Schenker T, Lach C, Kessler B, Calderara S, Trueb B. 1994. A Novel Gtp-Binding Protein Which Is Selectively Repressed in Sv40-Transformed Fibroblasts. *J Biol Chem* 269: 25447-25453.
2. Li B, Trueb B. 2000. DRG represents a family of two closely related GTP-binding proteins. *Biochim Biophys Acta*. 1491: 196-204.
3. Song H, Kim SI, Ko MS, Kim HJ, Heo JC, Lee HJ, Lee HS, Han IS, Kwack K, Park JW. 2004. Overexpression of DRG2 increases G2/M phase cells and decreases sensitivity to nocodazole-induced apoptosis. *Journal of Biochemistry* 135: 331-335
4. Ko MS, Lee UH, Kim SI, Kim HJ, Park JJ, Cha SJ, Kim SB, Song H, Chung DK, Han IS, Kwack K, Park JW. 2004. Overexpression of DRG2 suppresses the growth of Jurkat T cells but does not induce apoptosis. *Arch Biochem Biophys*. 422: 137-144
5. Ko MS, Kim HJ, Kim HK, Yoon NA, Lee UH, Lee SC, Chung DK, Lee BJ, Suh JH, Cho WJ, Park JW. 2014. Developmentally regulated GTP-binding protein 2 ameliorates EAE by suppressing the development of TH17 cells. *Clin Immunol*. 150: 225-235.
6. Mani M, Lee UH, Yoon NA, Kim HJ, Ko MS, Seol W, Joe Y, Chung HT, Lee BJ, Moon CH, Cho WJ, Park JW. 2016. Developmentally regulated GTP-binding protein 2 coordinates Rab5 activity and transferrin recycling. *Molecular Biology of the Cell*. 27(2): 334-348
7. Mani M, Thao DT, Kim BC, Lee UH, Kim DJ, Jang SH, Back SH, Lee BJ, Cho WJ, Han IS, Park JW. 2019. DRG2 knockdown induces Golgi fragmentation via GSK3 β phosphorylation and microtubule stabilization. *Biochim Biophys Acta Mol Cell Res*. 1866(9): 1463-1474
8. Doble, B.W. & Woodgett, J.R. 2003. GSK-3: tricks of the trade for a multi-tasking kinase. *J. Cell Sci*. **116**: 1175–1186.

9. Martin M, Rehani K, Jope RS, Michalek SM. 2005. Toll-like receptor-mediated cytokine production is differentially regulated by glycogen synthase kinase 3. *Nat Immunol.* 6:777–784.
10. Hu, X. et al. 2006. IFN-gamma suppresses IL-10 production and synergizes with TLR2 by regulating GSK3 and CREB/AP-1 proteins. *Immunity.* 24: 563–574.
11. Beurel, E., Michalek, S.M. & Jope, R.S. 2010. Innate and adaptive immune responses regulated by glycogen synthase kinase-3 (GSK3). *Trends Immunol.* 31: 24–31.
12. Steinbrecher, K.A., Wilson, W., Cogswell, P.C. & Baldwin, A.S. 2005. Glycogen synthase kinase 3 β functions to specify gene-specific, NF- κ B-dependent transcription. *Mol. Cell. Biol.* 25: 8444–8455.
13. Buss, H. et al. 2004. Phosphorylation of serine 468 by GSK-3 β negatively regulates basal p65 NF- κ B activity. *J. Biol. Chem.* 279: 49571–49574.
14. Saijo, K. et al. 2009. A Nurr1/CoREST pathway in microglia and astrocytes protects dopaminergic neurons from inflammation-induced death. *Cell.* 137: 47–59.
15. Takada, Y. et al. 2004. Genetic deletion of glycogen synthase kinase-3 β abrogates activation of I κ B α kinase, JNK, Akt, and p44/p42 MAPK but potentiates apoptosis induced by tumor necrosis factor. *J. Biol. Chem.* 279: 39541–39554.
16. Hoeflich, K.P. et al. 2000. Requirement for glycogen synthase kinase-3 β in cell survival and NF- κ B activation. *Nature.* 406: 86–90.
17. Rinnab, L. et al. 2008. Inhibition of glycogen synthase kinase-3 in androgen-responsive prostate cancer cell lines: are GSK inhibitors therapeutically useful? *Neoplasia.* 10: 624–634.
18. Viatour P, Merville MP, Bours V, Chariot A. 2005. Phosphorylation of NF- κ B and I κ B proteins. Implications in cancer and inflammation.

Trends Biochem Sci. 30: 43-52

19. Ghosh S, Hayden MS. 2008. New regulators of NF-kappa B in inflammation. Nat Rev Immunol. 8: 837-848.
20. Medunjanin, S. et al. 2016. GSK-3 β controls NF-kappaB activity via IKK γ /NEMO. Sci. Rep. 6, 38553; doi: 10.1038/srep38553.
21. Baldwin AS Jr. 1996. The NF-kappa B and I kappa B proteins: new discoveries and insights. Annu Rev Immunol. 14: 649-83.
22. Rothwarf, D. M., Zandi, E., Natoli, G. & Karin, M. 1998. IKK-gama is an essential regulatory subunit of the IkappaB kinase complex. Nature. 395: 297–300.
23. Hayden, M. S. & Ghosh, S. 2012. NF-kappaB, the first quarter-century: remarkable progress and outstanding questions. Genes Dev. 26: 203–234.
24. Posfay-Barbe KM, Wald ER. 2009. Listeriosis. Semin. Fetal Neonatal. Med. 14: 228-233.
25. Vazquez-Boland JA, Kuhn M, Berche P, Chakraborty T, Dominguez-Bernal G, Goebel W, Gonzalez-Zorn B, Wehland J, Kreft J. 2001. Listeria pathogenesis and molecular virulence determinants. Clin Microbiol Rev. 14: 584-640.
26. Corr, S. C. & O'Neill, L. A. 2009. Listeria monocytogenes infection in the face of innate immunity. Cell. Microbiol. 11: 703–709.
27. Witte CE, Archer KA, Rae CS, Sauer JD, Woodward JJ, et al. 2012. Innate immune pathways triggered by Listeria monocytogenes and their role in the induction of cell-mediated immunity. Advances in immunology. 113: 135–156.
28. Leber JH, Crimmins GT, Raghavan S, Meyer-Morse NP, Cox JS, et al. 2008. Distinct TLR- and NLR-mediated transcriptional responses to an intracellular pathogen. PLoS Pathog 4: e6.
29. Chatterjee SS, et al. 2006. Intracellular gene expression profile of *Listeria*

- monocytogenes*. *Infect Immun*. 74: 1323–1338.
30. Baldwin DN, Vanchinathan V, Brown PO, Theriot JA. 2003. A gene-expression program reflecting the innate immune response of cultured intestinal epithelial cells to infection by *Listeria monocytogenes*. *Genome Biol*. 4: R2.
 31. Lecuit M, Sonnenburg JL, Cossart P, Gordon JI .2007. Functional genomic studies of the intestinal response to a foodborne enteropathogen in a humanized gnotobiotic mouse model. *J Biol Chem*. 282: 15065–15072.
 32. Van Rooijen, N., Sanders, A., & van den Berg, T. K. 1996. Apoptosis of macrophages induced by liposome-mediated intracellular delivery of clodronate and propamidine. *Journal of immunological methods*. 193(1): 93-99.
 33. Westcott, M. M., C. J. Henry, A. S. Cook, K. W. Grant, and E. M. Hiltbold. 2007. Differential susceptibility of bone marrow-derived dendritic cells and macrophages to productive infection with *Listeria monocytogenes*. *Cell Microbiol*. 9: 1397-1411.
 34. Pils, S., T. Schmitter, F. Neske, and C. R. Hauck. 2006. Quantification of bacterial invasion into adherent cells by flow cytometry. *J. Microbiol. Methods* 65: 301–310.
 35. Libermann TA, Baltimore D. 1990. Activation of interleukin-6 gene expression through the NF-kappa B transcription factor. *Mol Cell Biol*. 10(5): 2327-34.
 36. Shakhov AN, Collart MA, Vassalli P, Nedospasov SA, Jongeneel CV. 1990. Kappa B-type enhancers are involved in lipopolysaccharide-mediated transcriptional activation of the tumor necrosis factor alpha gene in primary macrophages. *J Exp Med*. 171(1): 35-47.
 37. Hoefflich, K.P. et al. 2000. Requirement for glycogen synthase kinase-3 β in cell survival and NF- κ B activation. *Nature*. 406: 86–90.

38. Serbina, N. V. & Pamer, E. G. 2006. Monocyte emigration from bone marrow during bacterial infection requires signals mediated by chemokine receptor CCR2. *Nature Immunol.* 7: 311–317.
39. Conlan, J. W. & North, R. J. 1994. Neutrophils are essential for early anti-*Listeria* defense in the liver, but not in the spleen or peritoneal cavity, as revealed by a granulocyte-depleting monoclonal antibody. *J. Exp. Med.* 179: 259–268.
40. Van Rooijen, N., & Sanders, A. 1994. Liposome mediated depletion of macrophages: mechanism of action, preparation of liposomes and applications. *Journal of immunological methods.* 174(1-2): 83-93.
41. Cohen JJ, Scheimer HN, Claman HN, Oronsky AL. 1989. Anti-inflammatory steroid action. San Diego: Academic Press. Basic and clinical aspects; pp. 111–31.
42. Schwiebert LA, Beck LA, Stellato C, Bickel CA, Bochner BS, Schleimer RP. 1996. Glucocorticosteroid inhibition of cytokine production: relevance to antiallergic actions. *J Allergy Clin Immunol.* 97:143–52
43. K. De Bosscher et al. 2000. Glucocorticoids repress NF-kappaB-driven genes by disturbing the interaction of p65 with the basal transcription machinery, irrespective of coactivator levels in the cell. *Proc. Natl. Acad. Sci. U.S.A.* 97: 3919–3924.
44. Cain, D.W. and Cidlowski, J.A. (2017) Immune regulation by glucocorticoids. *Nat. Rev. Immunol.* 17: 233–247.
45. Gordon S. 2002. Pattern recognition receptors: doubling up for the innate immune response. *Cell.* 27: 927-930
46. Buchmeier, N. A. & Schreiber, R. D. 1985. Requirement of endogenous interferon- γ production for resolution of *Listeria monocytogenes* infection. *Proc. Natl Acad. Sci. USA* 82: 7404–7408.
47. Havell, E. A. 1989. Evidence that tumor necrosis factor has an important

- role in antibacterial resistance. *J. Immunol.* 143: 2894–2899.
48. Ehlers, S. et al. 2003. The lymphotoxin receptor is critically involved in controlling infections with the intracellular pathogens *Mycobacterium tuberculosis* and *Listeria monocytogenes*. *J. Immunol.* 170: 5210–5218.
49. Scheller J., A. Chalaris, D. Schmidt-Arras, S. Rose-John. 2011. The pro- and anti-inflammatory properties of the cytokine interleukin-6. *Biochim. Biophys. Acta* 1813: 878–888.
50. Chalaris A., C. Garbers, B. Rabe, S. Rose-John, J. Scheller. 2011. The soluble interleukin 6 receptor: generation and role in inflammation and cancer. *Eur. J. Cell Biol.* 90: 484–494
51. Kishimoto T., S. Akira, M. Narazaki, T. Taga. 1995. Interleukin-6 family of cytokines and gp130. *Blood* 86: 1243–1254.
52. Kopf M., H. Baumann, G. Freer, M. Freudenberg, M. Lamers, T. Kishimoto, R. Zinkernagel, H. Bluethmann, G. Köhler. 1994. Impaired immune and acute-phase responses in interleukin-6-deficient mice. *Nature* 368: 339–342.
53. Dalrymple S.A., L.A. Lucian, R. Slattery, T. McNeil, D.M. Aud, S. Fuchino, F. Lee, R. Murray. 1995. Interleukin-6-deficient mice are highly susceptible to *Listeria monocytogenes* infection: correlation with inefficient neutrophilia. *Infect. Immun.* 63: 2262–2268.
54. Liu Z., R. J. Simpson, C. Cheers. 1995. Interaction of interleukin-6, tumor necrosis factor and interleukin-1 during *Listeria* infection. *Immunology* 85: 562-567.
55. Nakane A., A. Numata, T. Minagawa. 1992. Endogenous tumor necrosis factor, interleukin-6, and γ interferon levels during *Listeria monocytogenes* infection in mice. *Infect. Immun.* 60: 523–528.
56. Ehlers S., M. E. Mielke, T. Blankenstein, H. Hahn. 1992. Kinetic analysis of cytokine gene expression in the livers of naive and immune mice infected with *Listeria monocytogenes*: the immediate early phase in innate resistance and acquired immunity. *J. Immunol.* 149: 3016–3022

57. Bettelli E., Y. Carrier, W. Gao, T. Korn, T.B. Strom, M. Oukka, H.L. Weiner, V. K. Kuchroo. 2006. Reciprocal developmental pathways for the generation of pathogenic effector T_H17 and regulatory T cells. *Nature* 441: 235–238.
58. Weaver C. T., R. D. Hatton, P. R. Mangan, L. E. Harrington. 2007. IL-17 family cytokines and the expanding diversity of effector T cell lineages. *Annu. Rev. Immunol.* 25: 821–852.
59. Dube P. H., S. A. Handley, J. Lewis, V. L. Miller. 2004. Protective role of interleukin-6 during *Yersinia enterocolitica* infection is mediated through the modulation of inflammatory cytokines. *Infect. Immun.* 72: 3561–3570.
60. LeBlanc R.A., L. Pesnicak, E.S. Cabral, M. Godleski, S.E. Straus. 1999. Lack of interleukin-6 (IL-6) enhances susceptibility to infection but does not alter latency or reactivation of herpes simplex virus type 1 in IL-6 knockout mice. *J. Virol.* 73: 8145–8151.
61. Dalrymple S.A., R. Slattery, D.M. Aud, M. Krishna, L.A. Lucian, R. Murray. 1996. Interleukin-6 is required for a protective immune response to systemic *Escherichia coli* infection. *Infect. Immun.* 64: 3231–3235.
62. Medunjanin, S., Schleithoff, L., Fiegehenn, C. *et al.* 2016 GSK-3 β controls NF-kappaB activity via IKK γ /NEMO. *Sci Rep* 6: 38553.
63. Bancroft GJ, Schreiber RD, Unanue ER. 1991. Natural immunity: a T-cell-independent pathway of macrophage activation, defined in the SCID mouse. *Immunol Rev.* 124: 5–24.
64. Bhardwaj V, Kanagawa O, Swanson PE, Unanue ER. 1998. Chronic Listeria infection in SCID mice: requirements for the carrier state and the dual role of T cells in transferring protection or suppression. *J Immunol.* 160: 376–384.
65. Pamer E. G. 2004. Immune responses to Listeria monocytogenes. *Nat Rev Immunol.* 4: 812–823.
66. Unanue ER. 1997. Studies in listeriosis show the strong symbiosis between the innate cellular system and the T-cell response. *Immunol Rev.* 158:11-25.

67. W Krenger. 1995. Polarized type 2 alloreactive CD4+ and CD8+ donor T cells fail to induce experimental acute graft-versus-host disease. *J Immunol.* 155:585.
68. Jamie E McInturff. 2005. The role of toll-like receptors in the pathogenesis and treatment of dermatological disease. *J Invest Dermatol.* 125(1):1-8.
69. Tamas Nemeth. 2020. Neutrophils as emerging therapeutic targets. *Nat Rev Drug Discov.* 19(4):253-275.
70. John R Teijaro. 2011. Endothelial cells are central orchestrators of cytokine amplification during influenza virus infection. *Cell.* 146(6):980-91.
71. Nico Van Rooijen. 1994. Liposome mediated depletion of macrophages: mechanism of action, preparation of liposomes and applications. *Journal of immunological methods.* 174:83-93
72. Nico Van Rooijen. 1996. Apoptosis of macrophages induced by liposome-mediated intracellular delivery of clodronate and propamidine. *Journal of immunological methods.* 193:93-99
73. Jenkins. 1972. Hemopoietic colony studies. VI. Increased eosinophil colonies obtained by antigen pretreatment of irradiated mice reconstituted with bone marrow cells. *J. Cell Physiol.* 79:413-422.